Fall 1982

The Effects of Varying Fresh Water Discharge on Dispersion in an Estuarine Hydraulic Model of the Lafayette River, Norfolk, Virginia

Michael J. Jugan
Old Dominion University

THE EFFECTS OF VARYING FRESH WATER DISCHARGE ON DISPERSION IN AN ESTUARINE HYDRAULIC MODEL OF THE LAFAYETTE RIVER, NORFOLK, VIRGINIA

by

Michael J. Jugan
B.S., May 1977, Stockton State College

A Thesis Submitted to the Faculty of
Old Dominion University in Partial Fulfillment of the
Requirements for the Degree of

MASTER OF SCIENCE

OCEANOGRAPHY

OLD DOMINION UNIVERSITY
September 1982

Approved by:

Dr. Carvel H. Blair (Director)

ABSTRACT

THE EFFECTS OF VARYING FRESH WATER DISCHARGE
ON DISPERSION IN AN ESTUARINE HYDRAULIC MODEL
OF THE LAFAYETTE RIVER, NORFOLK, VIRGINIA

Michael J. Jugan
Old Dominion University, 1982
Director: Dr. Carvel H. Blair

Three experimental tests were conducted in the Lafayette River branch of the Chesapeake Bay Hydraulic Model, each successive test with an increase in the amount of fresh water discharged into the head of the river. This was done to study the response from varying river discharge on mixing parameters including the longitudinal dispersion coefficient (E).

The model generated a tide of constant range and period. Batch releases of Rhodamine WT dye were made in the model and sampled throughout the river for ten tidal cycles. Samples were taken simultaneously at selected high and low water slack.

The calculation of the Estuary Number, Estuarine Richardson Number, and the Hansen-Rattray Model showed that the degree of stratification increased with fresh water discharge. The results showed good agreement between experimental and theoretical results. There is evidence from the experimental data showing that trapping of dye in side embayments could be a major mechanism for estuarine mixing.

Three methods were used to calculate the slack water approximation of the longitudinal dispersion coefficient. The salinity intrusion method

showed that E varied directly with increased discharge. The dynamic relationship method had only a slight increase for the low water slack approximation. The change in moment method displayed irregular results. The values were not in good agreement for the different methods.

Half-life values were calculated from the total dye mass and the maximum dye concentration. No difference was found in the half-life values for the low and medium discharge runs, but a substantial decrease in time for the high discharge run.

DEDICATION

To my parents: Mr. and Mrs. Joseph Jugan

ACKNOWLEDGMENTS

I am deeply grateful to the director of my thesis committee, Dr. Carvel H. Blair. Without his patience and guidance, this project could not have been completed. He was always there for consultation and encouragement during the rough times. I owe him a great deal of thanks, he has helped me become a better scientist.

I would also like to thank the other two members of my thesis committee, Dr. Chet Grosch and Dr. George Hecker. They were both very helpful throughout the entire project. Commentaries from Dr. Donald Johnson, Dr. Ronald Johnson and Dr. David Tyler were much appreciated.

I would like to express my appreciation to the Virginia Sea Grant Program funded through the Virginia Graduate Marine Science Consortium. The Grant made it possible to conduct the model experiments and supported me throughout the project.

Much appreciation goes to the staff of the Chesapeake Bay Hydraulic Model. Especially to Dick Bruno, Ginny Pankow, and Mitch Granat of the U. S. Army Corps of Engineers. The staff of the model contractor, Acres American Inc., were also very helpful.

I am thankful to all the graduate students of the Department of Oceanography, especially to those in old Room 120: Dr. Cintia Piccolo and her husband, Dr. Gerardo Perillo, for their support and encouragement, as well as computer help; Dr. Im Sang Oh, for guiding me through some difficult computer problems; to Dave Timpy, Joe Bleicher, Beth

Hester and Greg Kopanski for being there when I needed moral support.

I would also like to thank Larry White for helping me gather some of the data at the model. Thanks also to Charlie and Juanita Farmer for helping me take the slides for my defense.

The staff of the computer center deserves a pat on the back for their friendly and helpful service.

I am very thankful to Bonnie Brown for her help in preparing the final figures for the report. My thanks go to Helen V. Donn for typing the final report.

Most of all, I am extremely grateful to my wife Laurie. She not only helped me collect data, but was always there when I needed a soft shoulder to lean on. Her love, understanding, and encouragement made it possible to complete the project.

TABLE OF CONTENTS

LIST OF TABLES

LIST OF FIGURES

CHAPTER 1.

INTRODUCTION

The increased demand for knowledge of pollutant mixing in rivers and estuaries in recent years has prompted extensive studies of estuarine mixing and longitudinal dispersion. A primary concern in water pollution control is the rate at which a pollutant spreads out and the decrease in the peak concentration as the pollutant is transported downstream (Peterson et al., 1974). Dispersion has been defined by Fisher (1973) as the spreading of marked fluid elements by the combined action of a velocity distribution and diffusion. Mass transfer processes in estuaries are very complex because of the oscillation of flow due to tidal action and salinity intrusion. Because of the importance of the dispersion coefficient (E), it is necessary to develop a method for calculating the rate of dispersion.

Little information is available pertaining to dispersion in an estuary with a horizontal density gradient. An accepted approach to evaluate the mixing properties is to inject a slug (batch release) of a conservative dye tracer and observe its spread with time. Hydraulic models have recently been used to evaluate the ability of a tidal estuary to study this process. Parameters such as tidal range and salinity distributions can be modeled well in distorted Froude models. However, little is known about the similitude of mass transport in a distorted model. The models are primarily built to study tide heights, currents, and salinity. There is great potential for using hydraulic models in the study of dispersion if the law of similitude is known.

1.1 Purpose of the Present Study

The primary purpose of the present study is to determine the effects of varying fresh water river discharge on dispersion in the Lafayette River branch of the Chesapeake Bay Hydraulic Model. A constant amplitude cosine tide was used to simulate a quasi-steady-state condition so that the river discharge can be modified to study different environmental conditions.

Various estuary classification methods were applied to the river data to examine what effect the added discharge had on the horizontal and vertical salinity gradients. The longitudinal dispersion coefficient was determined for salinity and dye concentration distributions using a one-dimemsional analysis.

1.2 Previous Investigations

The first analysis of dispersion (Taylor, 1954) concentrated on steady-state turbulent velocity shears in a constant density field. The one-dimensional dispersion equation introduced by Taylor to describe the dispersion in a steady pipe flow, has been used in rivers and estuaries by many investigators (Smith, 1976; Chatwin, 1980; Officer and Lynch, 1981; Holly, Harleman, and Fischer, 1970; Trackston and Krenkel, 1967). The equation uses only quantities averaged over the cross section and assumes that all mass flux other than by the mean flow velocity is proportional to the concentration gradient and the dispersion coefficient. Fischer (1967), and Holly et al. (1970), have shown that dispersion in rivers and estuaries can be caused by velocity gradients in both the vertical and transverse direction and that in estuaries, either direction may dominate. Harleman et al. (1966) have shown that where the vertical gradients are important, distorted

hydraulic models may greatly exaggerate dispersion. The actual coefficient (Fischer, 1971) that describes dispersion in an estuary must be larger than the coefficient calculated from either vertical or transverse gradients separately.

Engineering literature contains many reports on the determination of the longitudinal dispersion coefficient. Many have used the longitudinal salinity gradient and a corresponding fresh water flow (Harleman, 1971; Fischer, 1979). The result depends on whether the salinity field is observed at high or low water slack, or if the salinity distribution is in steady-state. Fischer (1979, Table 7.7) lists some of the observed prototype values of the dispersion coefficients from estuary experiments. The values range from 100-300 m^2/sec, which is a characteristic range for narrow estuaries. Low values of 10-50 m^2/sec are generally found in constant density portions of the estuary.

According to Taylor (1954), the variance of longitudinal particle displacement (σ^2) increases lineraly with time after the initial mixing is complete. Fischer (1968) uses the variance in the change in moment method where E is defined as one-half the time rate of change of the variance. Other studies using this method were presented by Fischer (1973, 1979), Ward (1974), Beltaos (1980), Peterson et al., (1974).

Several writers have suggested that a complete analysis of dispersion must include the effect of side embayments or dead zones. Valentine and Wood (1977, 1979) describe this analysis in a natural stream, where they concluded that the embayments play an important role in determining the initial period of mixing. Day (1973) studied dispersion and determined that the effect of the dead zones, even discounting the tails of the distribution, did not approach a normal

distribution. Other investigations concerning dead zones were by Beltaos (1980), Pritchard (1969), Thackston and Krenkel (1967), and Dronkers (1978).

Previous investigations of the Lafayette River were concerned with the hydrography, hydraulics, and mass transfer characteristics. Blair (1976) conducted hydrographical and tidal surveys as well as a mass transfer study in a hydraulic model and the prototype. Sisson (1976) applied a mathematical model to predict tidal elevation and current velocity. Farling (1976) used a finite difference model to study dispersion of a dye tracer. White (1972) looked at the salinity, temperature, and tidal profiles. Blair et al., (1976) investigated the flushing ability of the River.

Many investigations have used hydraulic models to compare dispersion coefficients in the model to those found in the prototype. Kuo et al., (1978, Table 3) lists some of the values calculated and shows good agreement between model and prototype in both homogeneous bodies and mixed estuaries. Studies were conducted in estuaries with a longitudinal salinity gradient (Blair, 1976; Harleman, 1976; and Sugimoto, 1974) but no studies were found that illustrate the effects of varying river discharge on dispersion.

CHAPTER 2.

THE MODEL

The Chesapeake Bay Hydraulic Model was constructed on Kent Island in Stevensville, Maryland, during the period of October 1974 to April 1976. It is a fixed bed distorted model molded in concrete to conform to bathymetric charts prior to 1970. The model covers the entire area of Chesapeake Bay and its tributaries to the head of the tide and the surrounding land to an elevation of 6.1 m (20 ft) above sea level (Figure 1). The model is enclosed in a 58681.5 m (14.5 acre) building to protect it from the weather and debris. The interior of the shelter is 329.4 m (1080 ft) long, 207.4 m (680 ft) wide, and 12.19 m (40 ft) high.

The model was built on the basis of the equality of model and prototype Froude numbers reflecting similitude of gravitational effects. The Froude number is the ratio of inertial to gravitational forces and is defined as:

$$F = \frac{U_f}{(g\ d)^{\frac{1}{2}}} \qquad (1)$$

where U_f = river discharge per unit area of cross-section ($=Q_f/A$)

g = acceleration of gravity

d = water depth

Therefore, once the modeler has selected either the depth scale or the velocity scale, the other scale is set. The geometric model to prototype scales for the Chesapeake Bay Model are 1:1000 horizontally, 1:100

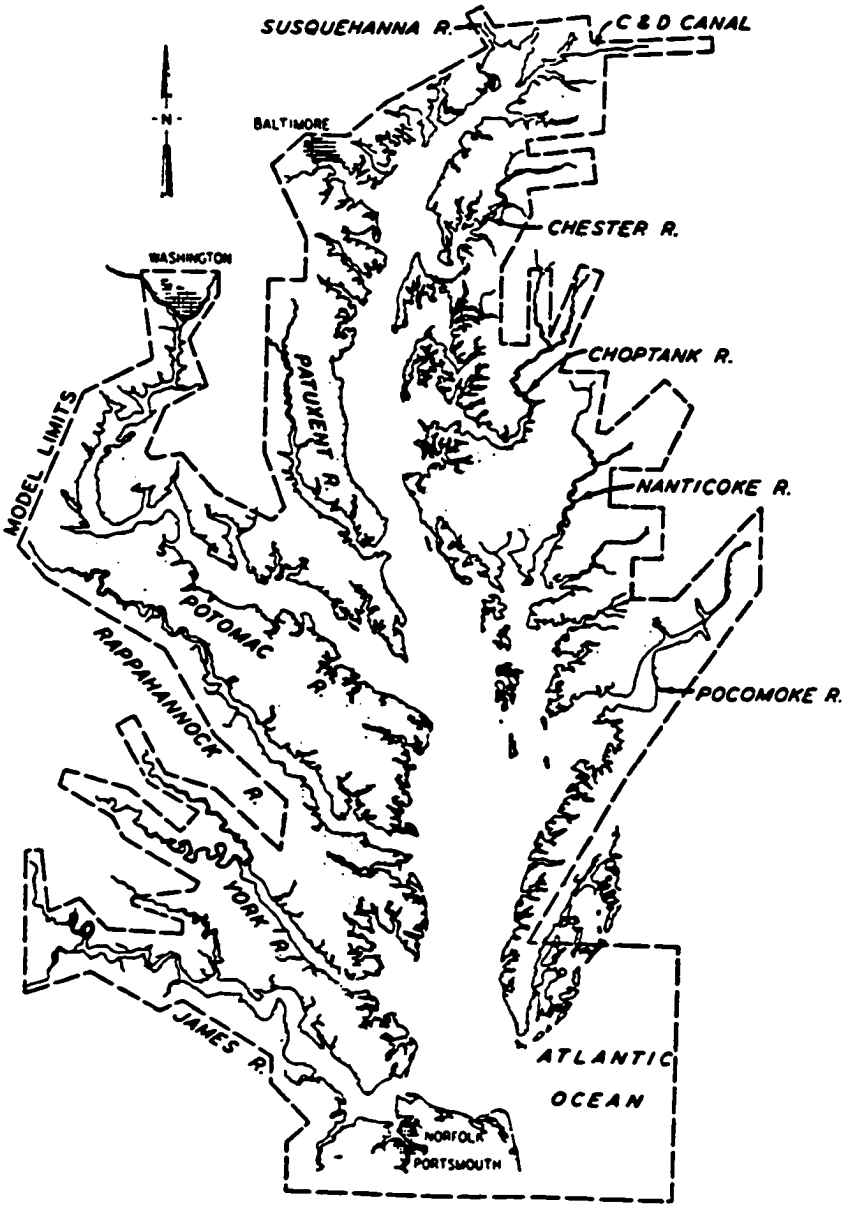

Figure 1. Area Covered by the Chesapeake Bay Hydraulic Model

vertically, yielding a vertical exaggeration of 10:1. The following scales are determined by the geometric relations and Froude law:

Characteristic	Ratio
Vertical Length	Dr = 1:100
Horizontal Length	Lr = 1:1000
Time	$Tr = Lr/Dr^{\frac{1}{2}} = 1:100$
Velocity	$Vr = Dr^{\frac{1}{2}} = 1:10$
Discharge	Qr = 1:1,000,000
Volume	$Lr^2Dr = 1:100,000,000$
Slope	Dr/Lr = 10:1
Dispersion Coefficient	$Er = Dr^{\frac{1}{2}}Lr = 1:10,000$

The model to prototype salinity ratio is unity. Additional bottom roughness is required in a distorted model in order to get the turbulent flow required to reproduce the proper tidal and salinity distributions and to reduce velocity caused by the greater slope ratio. In order to simulate the roughness needed, stainless steel strips 1.22 cm (0.5 in.) wide were embedded in the floor of the model. The strips can then be bent up or down until the proper tidal heights and velocities are obtained. In shallow areas (less than 2.5 cm or 1 in.) scratches were made in the cement to add roughness (Scheftner, et al., 1981).

The Lafayette River branch of the Chesapeake Bay Model was chosen for the present study (Figure 2). The river is located in Norfolk, Virginia, and is typical of the short tributaries of Chesapeake Bay. The length of the river in the model is 11 m (36.07 ft), with a maximum width of 0.8 m (2.62 ft). The main channel of the river branches 7 m (22.97 ft) from the mouth, with the north branch dividing again at 8.5 m (0.2 ft) with a mean depth of 0.012 m (0.04 ft). Table 1 lists some of the

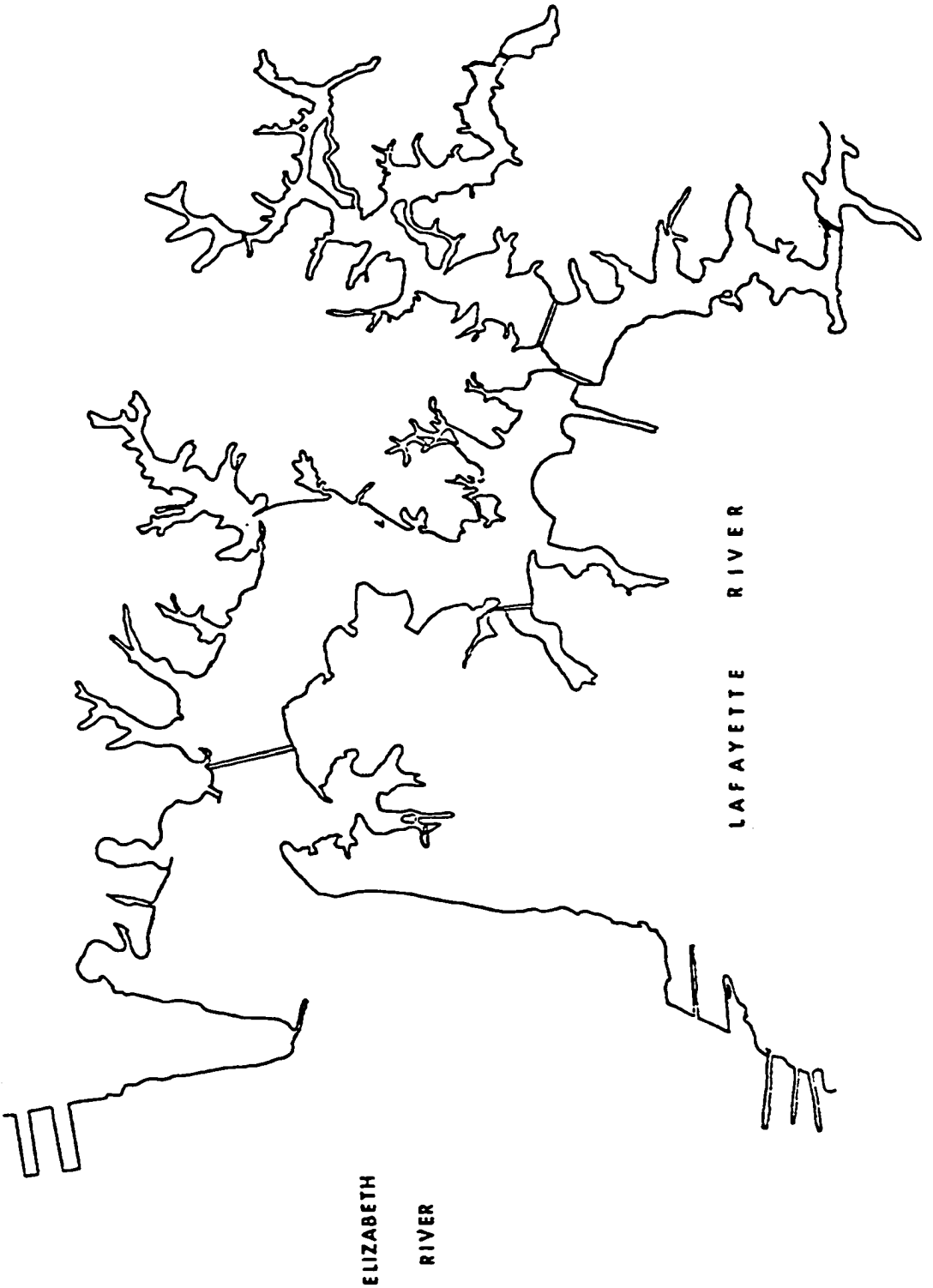

Figure 2. Study Area - Lafayette River

TABLE 1. MODEL PARAMETERS FOR THE LAFAYETTE RIVER

PARAMETER	RATIO	MODEL		PROTOTYPE	
CHANNEL LENGTH	1/1000	11 m	36 ft	11 km	36,089 ft
MEAN DEPTH	1/100	0.012 m	0.04 ft	1.2 m	4 ft
MEAN TIDAL RANGE	1/100	0.008 m	0.027 ft	0.8 m	2.7 ft
MAXIMUM VELOCITY	1/10	0.028 m/sec	0.091 ft/sec	0.28 m/sec	0.91 ft/sec
MAXIMUM WIDTH	1/1000	0.8 m	2.625 ft	800 m	2625 ft
TIDAL PERIOD	1/100	7.45 minutes		12.4 hours	
SALINITY	1/1	10/00		10/00	

major model parameters along with the equivalent prototype dimensions.

Model tides were controlled by a tide generator located at the Atlantic Ocean end of the model. The generator maintains the tide with the use of a Texas Instruments Model 960 minicomputer. The computer controls the amount of water pumped in during the flood tide and the gravity outflow for ebb tide. The source salinity was maintained at the ocean end of the model, which consists of a saturated brine solution mixed with granular salt (NaCl) and water. Skimming weirs are used to help maintain the model ocean at a constant salinity and water level by removing surface fresh water from the ocean area. The weirs are adjusted to draw off a discharge equal to the total fresh water inflow to the model. An air bubbler system is used throughout the model to enhance vertical mixing (Scheffner, et al., 1981).

Hydraulic models are valuable tools in investigating the physical phenomena of estuaries. The phenomena that can be reproduced or simulated in hydraulic models include tides, tidal currents, density currents, salinity, and mass dispersion. The magnitude, phase, and direction of the tidal current can be reproduced at a particular point as well as the longitudinal, lateral, vertical, and temporal velocity fields. The same is also true for salinity. Therefore, a physical model can provide a three-dimensional, time varying representation of the hydraulic and salinity fields of an estuary (Hudson, 1979).

There are many advantages and disadvantages of using hydraulic models. Once the model is constructed and verified, it is easier and faster to initiate changes and test the effects in a model than the prototype. The cost of such procedures is also substantially less than extensive prototype testing. The length of a model cycle is much

reduced; a 12 hour 50 minute tidal cycle in the prototype can be duplicated in 7 minutes and 37 seconds in the model.

Physical factors such as the tide and river discharge can be controlled in the model to simulate many prototype conditions. A hydraulic model is capable of simulating fluid flows with various densities in 3-dimensions (Hudson, 1979). Mathematical models could possibly simulate this flow but it is not often practical due to the huge amount of computer memory required. Models are also highly useful to visually demonstrate alternative plans of improvement, while providing the necessary understandable information by observation.

Physical scale models have been used to provide input to mathematical models. Scale models provide boundary and initial conditions as well as discharge coefficients for mathematical models. In addition, physical scale modeling is used to obtain dispersion coefficients which are used in mathematical models to simulate tidal transport phenomena. Mathematical models are often easily verified by using existing hydraulic models (Simmons, Harrison, and Huval, 1971).

Hydraulic models also have some shortcomings. Not the least is the initial great cost of construction and verification. It is difficult to study wind effects and suspended-sediment concentrations in a hydraulic model. Phenomena which cannot be reproduced in a fixed bed hydraulic model include shoreline erosion, bottom scour, decay of pollutants, chemical interactions, turbidity, refraction, and diffraction of short-period waves, and biological processes (Hudson et al., 1979).

Using a distorted scale serves the essential purpose of making the model flow turbulent, but it also changes the longitudinal slope of the

channels and distorts rates of vertical and transverse mixing. The tendency of the model flow to be too fast, because of the increased slope, must be resisted by adding friction to the channels. Vertical metal strips are arranged over the entire model to provide extra friction to counteract the distorted channel and water surface slopes. The vertical strips do stimulate mixing, but there is no certainty that the mixing rates generated by the strips in the model and the rates generated by the tidal currents and bottom friction in the prototype will be the same (Fischer, 1979). The cross-sectional velocity distribution is not usually well enough known in the prototype to be tested in the model, and local rates of transverse and vertical mixing are usually not tested at all.

Even though models are often used to study near-source dispersion problems, it is not customary to attempt verification of local turbulent mixing. In a stratified model, verification of the local vertical salinity gradient implies verification of the rate of vertical mixing. It implies nothing about the rates of transverse mixing. No data available concerning the ability of a stratified model to stimulate transverse mixing have been found (Fischer, 1979).

Ippen (1966) implies that hydraulic models should not be looked upon as a substitute for field and analytical studies, but rather as an aid in such studies by contributing information which cannot be obtained accordingly by other means.

CHAPTER 3.

EXPERIMENTAL PROCEDURES

Three experimental tests were conducted in the Chesapeake Bay Hydraulic Model, each successive experiment with an increase in the amount of fresh water discharged into the head of the branches of the Lafayette River. This was done to simulate three different environmental conditions of normal, above normal, and heavy rainfall. The model tide was running and in approximate dynamic equilibrium before testing started. A clock was started when low water slack was recorded at station L5 (noted as LWO). Samples were taken at selected low water and high water slacks for ten tidal cycles or an equivalent of five prototype days (see Table 2). Sampling stations were located one meter (3.28 ft.) apart starting at the mouth of the river and proceeding up each branch (Figure 3). One side embayment 5.5 m (18.03 ft.) from the mouth of the river was also sampled. Surface samples were taken at all stations, with bottom samples taken at three of the deeper locations (stations L2, L4, and L7). The model tides were operated and samples read by Acres American Inc.,personnel, service contractors for the Corps of Engineers. Old Dominion University personnel regulated river discharge, conducted dye tracer experiments, and collected all samples.

3.1 River Discharge

Fresh water was added to the model from the major tributaries of Chesapeake Bay as well as from the two branches of the Lafayette River. The total bay discharge was 0.008871 m^3/sec (0.31328 $ft.^3$/sec) at the beginning of the experiment (Acres American Inc., 1981). The only

TABLE 2. SAMPLING TIMES FOR RUNS B, C, AND D

TIDAL EVENT	ELAPSED TIME (SEC)	NOTE
LW 0	0	CLOCK STARTED
HW 1	223	BACKGROUND TAKEN
LW 1	447	DYE RELEASED
HW 2 *	670	SAMPLING STARTED
LW 2	894	
HW 4	1564	
LW 4	1788	
HW 6	2458	
LW 6	2682	
HW 8	3352	
LW 8	3576	
HW 9	3799	
HW 10	4246	
LW 10	4470	

* FOR RUN D, HW 3 WAS SAMPLED (1117 sec)

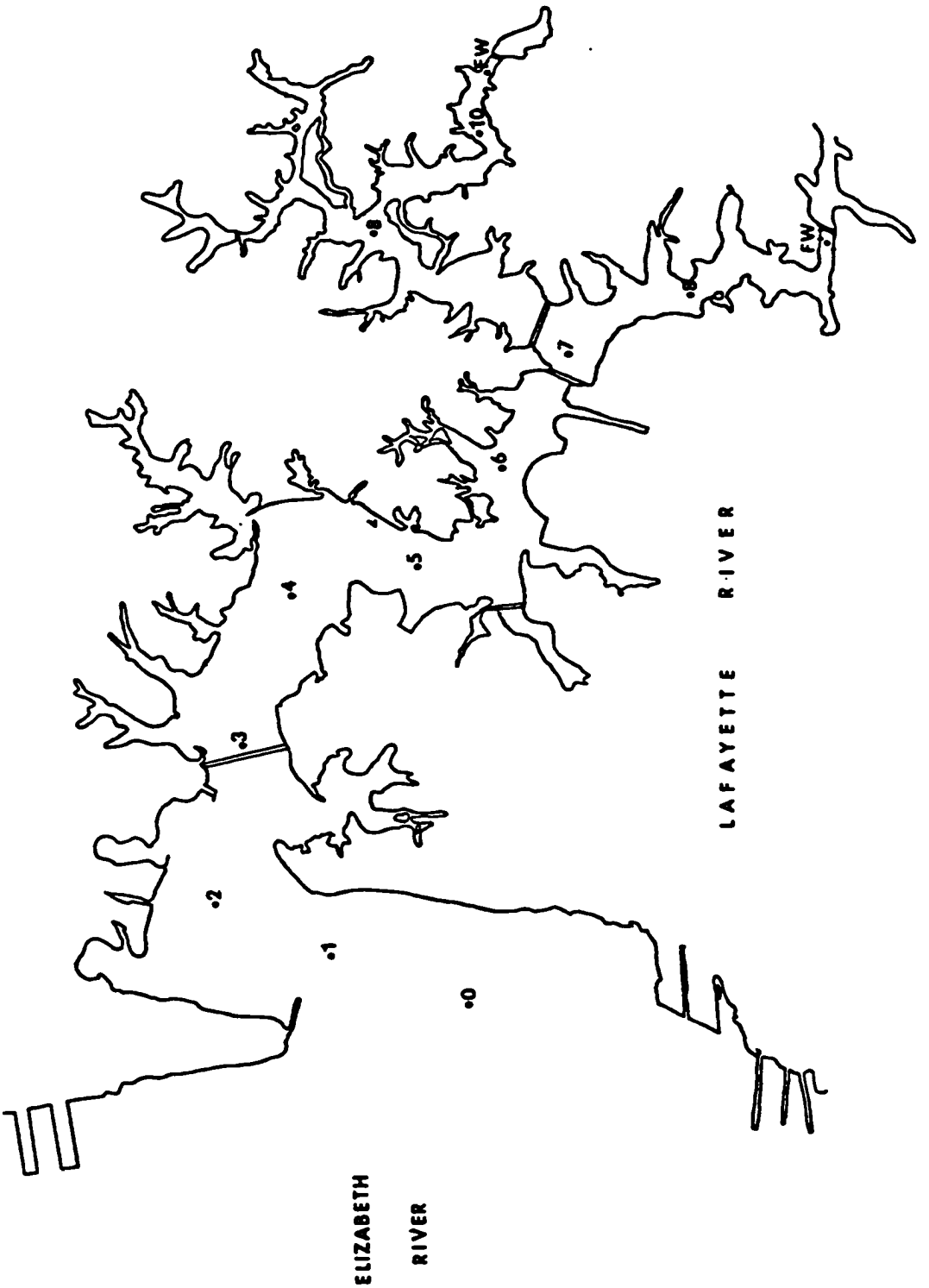

Figure 3. Lafayette River Sampling Stations and Fresh Water Discharge Locations

addition to the bay discharge after the experiments started was from the branches of the Lafayette River.

A constant head tank using gravity feed was used to discharge fresh water into the branches of the Lafayette River. The fresh water flow into the model was controlled with a Dyer Roto Meter. The Roto Meters were calibrated before and after each experiment. There was some drift in the flow meters which could have added small errors to the data. Discharge rates will be presented in a later chapter.

3.2 Model Tide

In order to limit the present study to the effects of varying river discharge, the model tide was set to simulate quasi-steady-state conditions. The M_2 tidal constituent was used to generate a reproducible cosine tide of constant tidal range and period, therefore simulating quasi-steady-state conditions. The M_2 tide is based on the following relationship:

$$h\,(t) = A_0 + a \cos\left(\frac{2\pi\ \omega t}{360} - \frac{2\pi\varepsilon}{360}\right) \qquad (2)$$

where $h(t)$ = M_2 tide height at time t

t = time

A_0 = Mean height above reference datum

a = M_2 amplitude

ω = M_2 constituent angular velocity

ε = Phase angle in degrees measured from equilibrium tide passing Greenwich at Ø hour GMT

The experiments were run with an ocean high water of +0.396 cm (+0.013 ft.) and low water of -0.518 cm (-0.017 ft.) yielding a tidal

range at the mouth of the Lafayette River of 0.914 cm (0.027 ft.) or a prototype equivalent tidal range of 91.4 cm (2.7 ft.) (Figure 4).

The tide was recorded at the ocean and at Sewells Point with a high-precision water level detector and relayed to the main computer. The sensors were designed and built by the Waterways Experiment Station and use an air-capacitance system. A strip chart recorder was used at Sewells Point to monitor the shape of the cosine tide and to record the elapsed tidal cycles. A point gauge was used to measure the tidal elevations at station L4.

3.3 Dye Injection

Batch releases of Rhodamine WT fluorescent dye were made across the channel 5 m (16.39 ft.) from the mouth of the Lafayette River at station L5 for all three experiments. The release was made at low water slack one tidal cycle after the running clock was started (LW 1). The release consisted of 10 ml of 1.85×10^{-4} mass concentration of Rhodamine WT dye, assuming a 20% manufacturers source concentration. Rhodamine WT dye is a conservative dye that was designed for use in model studies.

3.4 Dye Sampling Equipment

In order to determine the dye concentration in the water column after release, vacuum sampling equipment supplied by model personnel was used. The equipment consisted of thin plastic tubes mounted on a rod at the desired depth for all sampling stations. The tubes were connected through a vacuum pump to 10 ml test tubes. The pump was activated at the desired sampling time filling all test tubes simultaneously.

The dye concentration of each sample was measured by the model operator, Acres American Inc. using Turner Designs Model 10-000

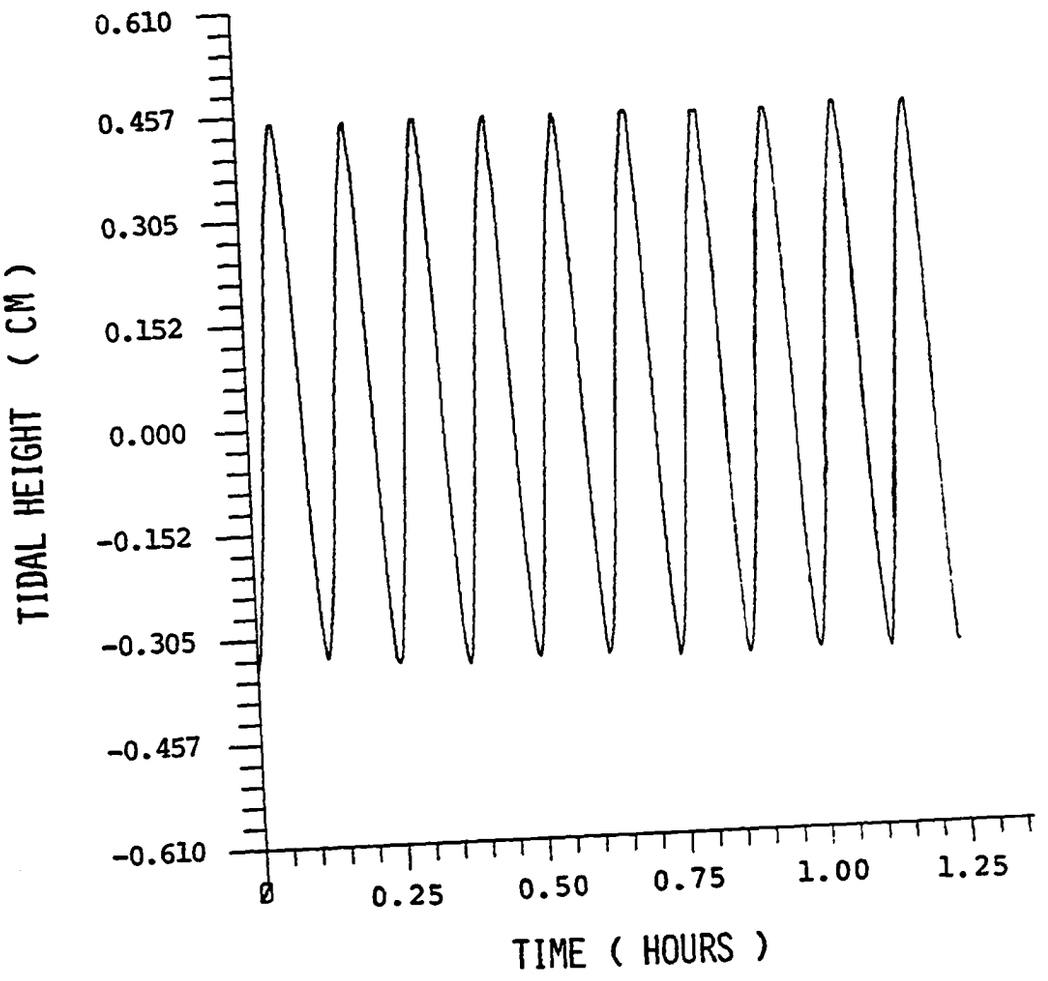

Figure 4. Model Tidal Height for Run B
Measured at Sewells Point

Fluorometers. The Fluorometer provided a millivolt reading which was recorded on a data logging cassette. The cassette provided the data in the format required for the Texas Instruments Model 980 mini-computer used for data reduction. The dye concentration in parts per billion (ppb) were then determined by using calibration curves from a set of 13 different dye standards (Acres American Inc., 1981).

3.5 Velocity Measurements

Model current velocity measurements were taken using a miniature Price-type pygmy current meter. The current meter was placed at approximately the mid-water depth at station L4. Velocities were obtained by counting the number of revolutions made in a 10 second interval. This was repeated every 36 seconds (one hour prototype equivalent) for two tidal cycles during Run C. The meter was calibrated to ensure an accuracy of ±0.015 m/sec (±0.05 ft/sec).

Several attempts were made to use a Marsh-McBirney Model 523 electromagnetic current meter, but the model velocities were below the detectable limits of the current meter. There could also have been a problem due to the fact that the model is very shallow (less than 5 cm or 0.16 ft.) with metal strips which could affect the magnetic field around the probe.

3.6 Salinity Samples

Salinity samples were read by the model operator, Acres American Inc. All salinity samples were taken at the same time as the dye samples and analyzed on a Beckman Solumeter Model RA5. The Solumeters were calibrated using standards on the grams NaCl per kilogram basis (Acres American Inc., 1981).

CHAPTER 4.

COMPUTATIONAL PROCEDURES

4.1 Normalization of Data

The dye and salinity data collected from all three experiments were normalized in order to directly compare the results. A background dye sample collected at each station revealed that the Lafayette River was slightly fluorescent even before the dye releases. The background fluorescence was found to fit a linear approximation for all the data except in the shallow branches where the actual value was used (Figure 5). Therefore to get the actual dye concentration, it was necessary to subtract out the background fluorescent dye concentration (C_b) and divide by a normalization value (C_0). The normalization value was taken to be the maximum dye concentration value one tidal cycle after release (LW2). The following equation was used to get the actual normalized concentration of dye at a given point:

$$C(X,t) = \frac{C - C_b}{C_0 - C_b} \tag{3}$$

where C = Dye concentration (g/M^3)

C_b = Background dye concentration

C_0 = Normalization value

The salinity samples were normalized by dividing the measured value be the maximum value recorded at the mouth of the river by the following equation:

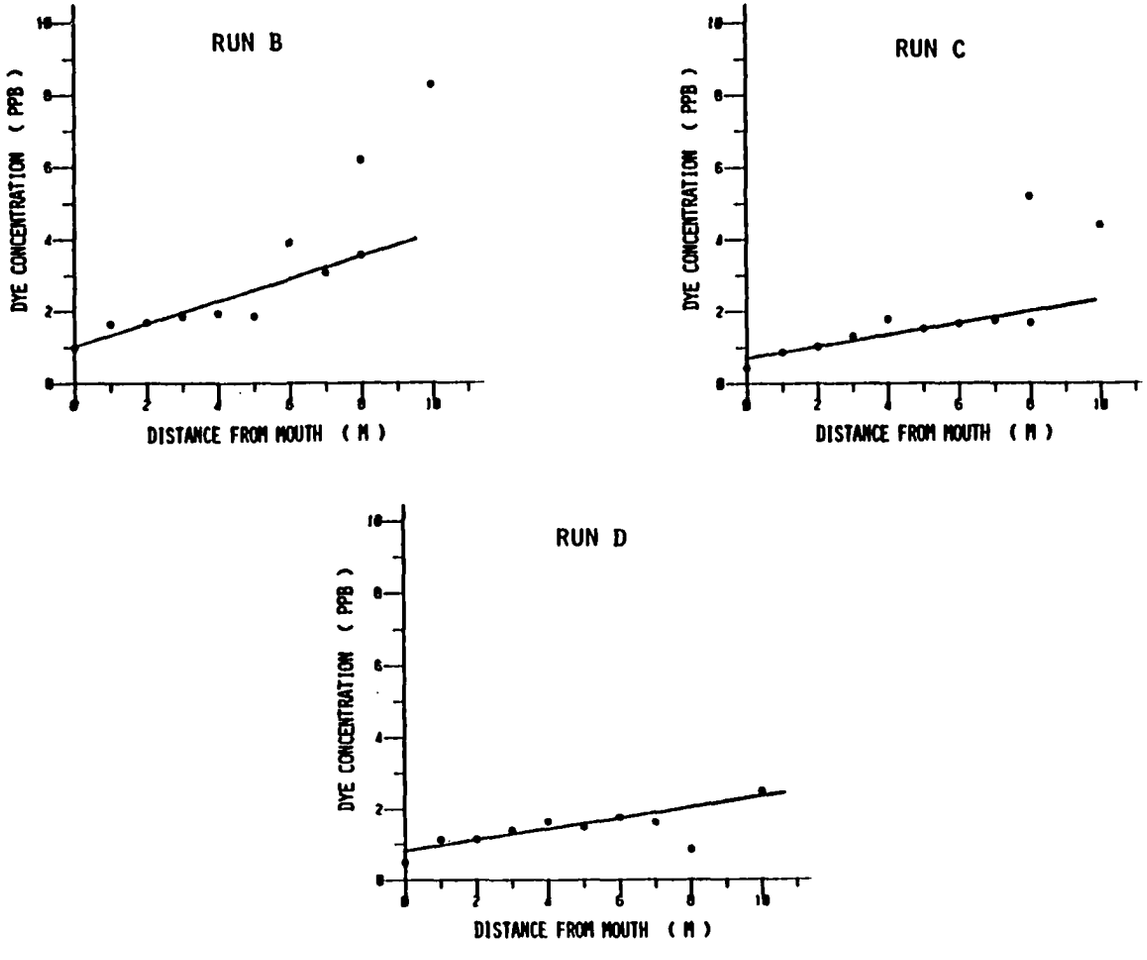

Figure 5. Background Fluorescent Dye Values Collected at HW 1

$$S(X,t) = \frac{S}{S_{max}} \tag{4}$$

where S = Local salinity

S_{max} = Maximum salinity at mouth of river

4.2 Estuary Number

Four classes of estuaries based on the relationship between tidal currents and river flow were found by Bowden (1967) and Pritchard (1967). The classification is based on the order of magnitude of the estuary number which is defined as:

$$N_e = \frac{P_T}{Q_f T} \tag{5}$$

where P_T = Tidal prism (= A Δh)

A = Mean water surface area

Δh = Change in tidal height from high to low water

Q_f = Fresh water discharge

T = Tidal period

When this ratio is small ($N_e \approx 1$) the stratification and circulation approximate a salt wedge. As the ratio becomes larger ($N_e \approx 10$ to 100) the estuary has the characteristics of a partially mixed estuary. Vertical homogeneity occurs when the ratio is very large ($N_e \approx 1000$).

4.3 Estuarine Richardson Number

In a study of mixing across an interface in an inclined channel, Ellison and Turner (1960), showed that the physically important parameters are the velocity and input of buoyancy per unit width. For

estuaries Fischer (1972) defined an estuarine Richardson number to show this relationship as follows:

$$R_{IE} = \frac{(\frac{\Delta\rho}{\rho})g\, Q_f}{W\ U_T^3} \qquad (6)$$

where $\frac{\Delta\rho}{\rho}$ = Difference in density of river and ocean

Q_f = Fresh water discharge

W = Channel width

U_T = rms tidal velocity

It expresses the ratio of the input of buoyancy per unit width of channel to the mixing power available from the tide (Fischer, 1979). This relationship is in analogy to what Ellison and Turner (1960) called the "Pipe Richardson Number".

If R_{IE} is large, the estuary is found to be highly stratified and the flow dominated by density currents. A small value of R_{IE} will indicate a well-mixed estuary and small density effects. Observations from real estuaries indicate that the transition from well mixed to stratified occurs in the range of $0.08<R_{IE}>0.8$ (Fischer, 1979). Therefore, the Estuarine Richardson Number is found to be a measure of the degree of stratification of an estuary (Fischer, 1972).

4.4 Hansen - Rattray Classification Model

Hansen and Rattray (1965, 1966) developed a way of classifying an estuary based on two parameters, circulation and stratification. They considered a partially mixed estuary of rectangular cross-section and sufficiently narrow to be laterally homogeneous. The classification

scheme used the central portion of the estuary where the vertical salinity stratification is nearly independent of position. Tidal currents are assumed to be the main cause of turbulent mixing, but have no effect on the net circulation of the estuary.

Hansen and Rattray (1965) developed the following equations which relate the distributions of salinity and horizontal current velocity to the controlling parameters:

$$\frac{U}{U_f} = -\frac{\partial \phi}{\partial \eta} \tag{7}$$

$$\frac{S}{S_0} = 1 + \beta \xi + \frac{\beta}{M}\left[\left(\eta - \frac{1}{2}\right) - \frac{1}{2}\left(\eta^2 - \frac{1}{3}\right) - \int_0^{\eta} \phi \, d\eta + \int_0^{\eta} \phi \, d\eta' \, d\eta\right] \tag{8}$$

and

$$\phi(\eta) = \frac{1}{2}(2 - 3\eta + \eta^3) - \frac{T}{4}(\eta - 2\eta^2 + \eta^3) - \frac{\beta Ra}{48}(\eta - 3\eta^3 + 2\eta^4) \tag{9}$$

where U = Horizontal velocity

ϕ = A stream function

η = Vertical coordinate (z/D)

β = Constant representing the diffusive fraction of the total upstream salt flux

ξ = Dimensionless horizontal coordinate ($=Rx/BDK_h$)

K_h, K_v = Horizontal and vertical turbulent diffusivities

B, D = Width and depth of the estuary

A_v = Vertical turbulent velocity

S = Time-mean salinity

S_0 = Sectional mean of S

R_a = Estuarine Rayleigh Number (gKS_0D^3/A_vK_h)

M = Tidal mixing parameter ($= K_vK_hB^2/k^2$)

$K = (1/\rho)(\partial\rho/\partial S)$

T = Dimensionless wind stress

R = River discharge rate

U_s = Net surface current

Equation (9) expresses the circulation as the sum of the river discharge mode, wind-stress mode, and gravitational-convection mode associated with the Rayleigh Number, which is the relationship of the potential energy to move a fluid to the kinetic energy. With no wind as in the present study, the velocity profile depends on the βRa term. As βRa increases, the density gradient increases and the flow becomes bi-directional for $\beta Ra \rightarrow 30$.

The diffusive factor β is obtained from the positive root of:

$$1680\, M(1-\beta) = (32 + 10T+T^2) + (76+14T)\left(\frac{Ra}{48}\right)\beta^2 + \frac{152}{3}\left(\frac{Ra}{48}\right)^2 \beta^3 \qquad (10)$$

The gradient parameter, β, represents the diffusive fraction of the total upstream salt flux (Hansen and Rattray, 1965).

The features of the mathematical model are best described by using dimensionless parameters. The circulation parameter (U_s/U_f) is defined as the ratio of the net surface current to the mean fresh water velocity through the section. The stratification parameter ($\partial S/S_0$) is defined as the ratio of the surface to bottom salinity difference to the mean salinity over the section. As $\beta \rightarrow 0$, diffusion becomes unimportant and the upstream salt flux is caused by gravitational convection (i.e., density driven circulation). When $\beta \rightarrow 1$, gravitational ceases and turbulent diffusion dominates. For values of β between 0.1 and 0.9, advective and diffusive fluxes are both important for the salt balance.

By using the mathematical model, Hansen and Rattray (1966) have identified seven types of estuaries using the two parameters and formed

a stratification-circulation diagram (Figure 6) entered with arguments of ($\partial S/S_0$) and (U_s/U_f). In type 1 the net flow is seaward at all depths and the upstream salt transfer is by diffusion. Type 1a is a typical well mixed estuary with a slight stratification, while type 1b has appreciable stratification. In type 2 the net flow reverses at depth and both advection and diffusion are important to the upstream salt flux, and corresponds to a partially mixed estuary. The stratifications of type 2a and 2b correspond to type 1a and 1b. In type 3 the salt transfer is dominated by advection. Type 3b estuaries have a lower layer that is so deep that the effect of the salinity gradient and circulation do not reach the bottom, as in a fjord. Type 4 is highly stratified like a salt wedge.

Since some of the parameters used in the mathematical model are not readily measurable, such as eddy coefficients for viscosity and diffusion, bulk parameters were defined which rely on the river flow, tide, and geomorphology. The main features of the bulk parameters have the dimensions of velocity. U_f is the river discharge per unit area of cross-section (Q_f/A), U_T is the root mean square (rms) tidal current speed ($\sqrt{2}/2\ U_{max}$). The densimetric Froude Number (F_m) expresses the ratio of fresh water river flow to potential for density-induced circulation and is defined as:

$$F_m = \frac{U_f}{\left(\left(\frac{\Delta\rho}{\rho}\right) g\ d\right)^{\frac{1}{2}}} \qquad (11)$$

where $\frac{\Delta\rho}{\rho}$ = Density difference between river and ocean

d = Water depth

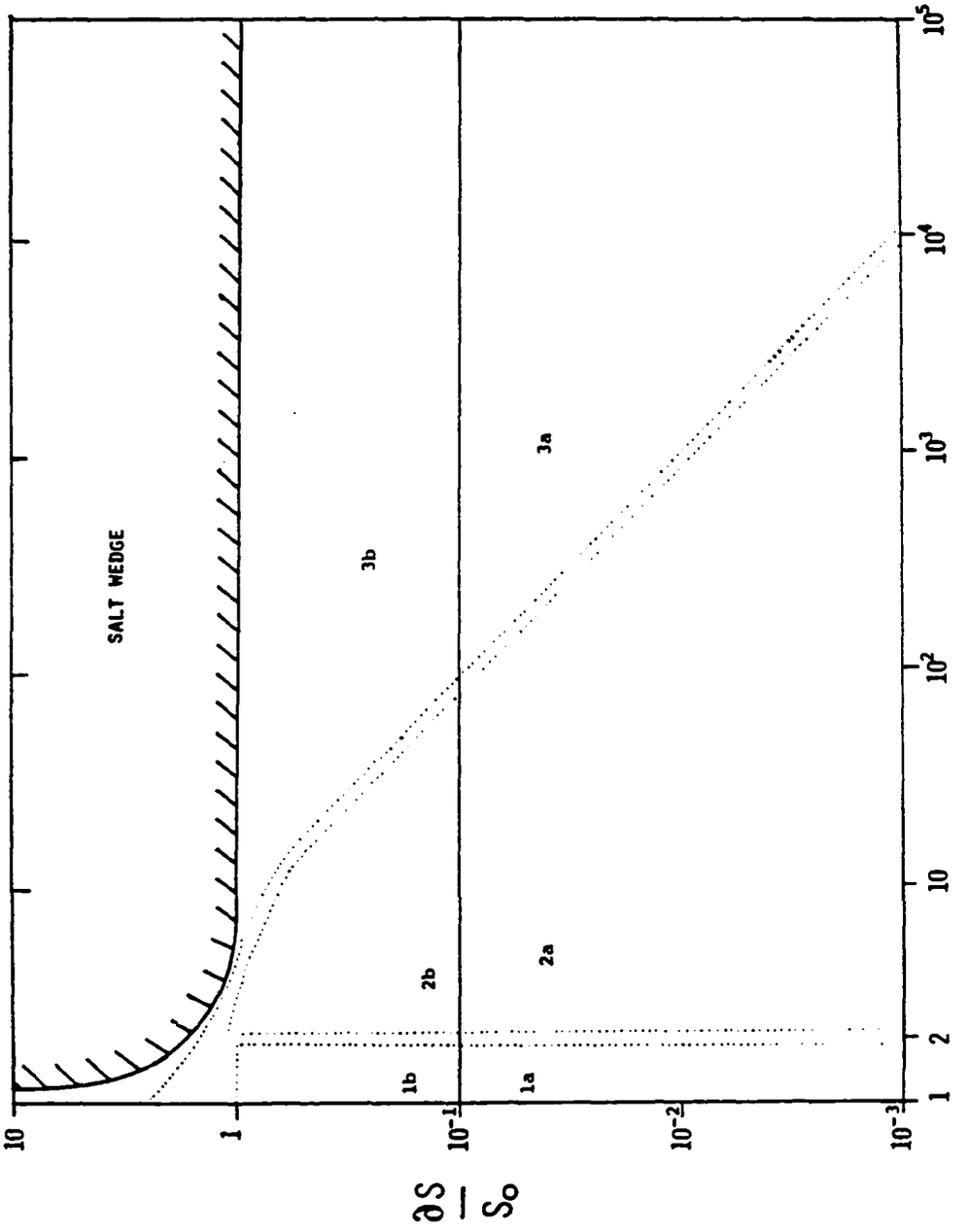

Figure 6. Hansen-Rattray Stratification-Circulation Diagram (after Hansen-Rattray, 1965)

The ratio $P=U_f/U_T$ is proportional to the flow ratio, and is found to be an adequate measure of the tidal mixing. The following bulk parameters were found from correlations with theoretical parameters:

$$Ra = 16\ F_m^{-3/4} \tag{12}$$

and

$$\frac{M}{\beta} = 0.05\ p^{-7/5} \tag{13}$$

Correlations for βRa less than 100 show uncertainty in distinguishing density effects from the influence of side boundaries on the velocity profiles. The correlations for large values of βRa with Fm is good.

Hansen and Rattray (1966) found that if the proposed parameters are adequate, then one has reason for using the model as a basis for estimation of complete vertical profiles of mean salinity and velocity in well-mixed and partially mixed estuaries.

4.5 Longitudinal Dispersion Coefficient by Salinity Intrusion

The following analysis to find the longitudinal dispersion coefficient by salinity intrusion, requires that the estuary be long and narrow with an identifiable channel axis, like the Lafayette River. The longitudinal dispersion coefficient can be found along the channel axis by combining all the dispersive mechanisms, such as by the tide and river, into a single dispersion coefficient. Fischer (1979) and Harleman (1971) express the "salt balance" in an estuary under quasi-steady-state conditions by the equation:

$$U_f S = E \frac{\partial S}{\partial X} \tag{14}$$

where $U_f = Q_f/A$

S = Local salinity

E = Longitudinal dispersion coefficient

Equation (14) states that the downstream advection of salt by the mean flow is in balance with the upstream transport by all other mechanisms. The magnitude of E is determined by observation of *in situ* tracers such as salinity (Fischer, 1979).

Solving the above equation for E yields:

$$E = \frac{U_f\ S}{\frac{\partial S}{\partial X}} \tag{15}$$

This equation can be used to obtain the longitudinal dispersion coefficient for either high water or low water slack depending on which salinity data is used (Harleman, 1971).

4.6 Longitudinal Dispersion Coefficient by Dynamic Relationship

In the fresh water region of the estuary, Harleman et al., (1966) found that the dispersion coefficient for the turbulent flow can be expressed by the relationship of the maximum cross-sectional velocity, Manning's "n", and the hydraulic radius by the following:

$$E_T = 100\ n\ U_{max}\ R_h^{5/6} \tag{16}$$

where n = Manning's n

U_{max} = Maximum velocity

R_h = Hydraulic radius ($\approx$d)

This equation is useful in quasi-steady-state conditions, but does not have the ability to predict the dispersion coefficient with varying

fresh water discharge.

In the saline region of a partially mixed estuary the dispersion coefficient is closely related to the density induced circulation. It is assumed that this density circulation will be the greatest in regions of a strong longitudinal salinity gradient ($\partial S/\partial X$). Thatcher and Harleman (1972) developed a dynamic relationship for the dispersion coefficient in an estuary that is well mixed. This relationship is formulated as:

$$E\ (X,t) = E_T + \left| K\ \frac{\partial S^0}{\partial X^0} \right| \tag{17}$$

where $S^0 = S/S_0$

S = Salinity

S_0 = Salinity at River mouth

$X^0 = X/L$

L = Length of estuary

$K = 0.002\ U_0 L\ N_{ed}^{-\frac{1}{4}}$

N_{ed} = Densimetric estuary number $\left(= \frac{P_T\ Fm^2}{Q_{f\ T}}\right)$

P_T = Tidal prism

F_m = Densimetric Froude number

T = Tidal period

Q_f = Fresh water discharge

U_0 = Maximum river velocity

E_T must be increased by the $K\ (\partial S/\partial X)$ term which accounts for additional dispersion due to the local salinity gradient. K has units of a dispersion coefficient and depends on the degree of stratification in the estuary. Equation (32) can be used to calculate either the high or low water slack approximation of the longitudinal dispersion coefficient, depending on which salinity data is used.

4.7 Longitudinal Dispersion Coefficient by the Change in Moment Method

Another way to compute E involves the time spreading of a dye tracer. The units of concentration of a dye tracer (C(X,t)) are usually given in terms of mass per cubic volume. Fischer (1979) prefers to apply dimensional analysis for a one dimensional approach. Since the process is assumed to be linear, the concentration must be proportional to the mass of dye introduced to the system. In one-dimension, the units of concentration are mass per unit length, therefore, forcing a one-dimensional fit to the data by dividing by some characteristic area, such as the cross-sectional area of each segment sampled.

New variables were defined to meet this criteria. M' is defined as the mass of dye in a river segment of length ΔX:

$$M'(X) = C(X,t)\ A(X)\ \Delta X \tag{18}$$

where $C(X,t)$ = Concentration of dye (g/M^3)

$A(X)$ = Cross-sectional area

ΔX = Axial length of segment

therefore, we can now define the one-dimensional concentration C' as;

$$C'(X,t) = \frac{M'(X)}{\Delta X} = C(X,t)\,A(X) \tag{19}$$

where the units are in mass per unit length.

This result can now be used to calculate the longitudinal dispersion coefficient by the moment method. Fischer (1979) defines the various moments of the concentration distribution are as follows:

$$\text{ZEROTH MOMENT} = M_0 = \int_{-\infty}^{\infty} C'(X,t)\,dx \tag{20}$$

$$\text{FIRST MOMENT} = M_1 = \int_{-\infty}^{\infty} XC'(X,t)\,dx \tag{21}$$

$$= M_1 = \int_{-\infty}^{\infty} XC'(X,t)\,dx$$

$$\text{SECOND MOMENT} = M_2 - \int_{-\infty}^{\infty} C(X,t)\,dx \tag{22}$$

The mean μ and variance σ^2 of the distribution are found from the moments by:

$$\mu = \frac{M_0}{M_1} \tag{23}$$

and

$$\sigma^2 = \int_{-\infty}^{\infty}(X-\mu)^2 \, C'(X,t) \, dx/M_0 = \left(\frac{M_2}{M_0}\right) - \mu^2 \tag{24}$$

Fischer (1979) uses the result of equations (21) and (22) to calculate the longitudinal dispersion coefficient by the following relation:

$$\frac{d\sigma^2}{dt} = 2E \tag{25}$$

or taking the dispersion coefficient as one-half the time rate of change of the variance σ^2 as:

$$E = \frac{1}{2}\frac{d\sigma^2}{dt} \tag{26}$$

This relation is found to be true not only for a normal distribution, but also for any concentration distribution, provided that the tracer is dispersing like the diffusion equation:

$$\frac{\partial C}{\partial t} = E\left(\frac{\partial^2 C}{\partial X^2}\right) \tag{27}$$

in a one-dimensional system of infinite extent and the concentration is zero at $X = \pm\infty$.

The change in moment method for the calculation of the longitudinal dispersion coefficient is theoretically exact but it is difficult to calculate the moments if the distribution has long tails. In using

concentration-time data, it must be assumed that as the dye cloud passes a sampling station, no dispersion is occurring. This assumption is reasonable for high flow rates but is questionable for low flow rates.

The variance of a distribution is assumed to increase linearly with time after a finite initial period has elapsed since the beginning of the dispersion process. This initial period is the time from dye injection required for complete transverse mixing to be complete and is known as the mixing time. The time after the mixing time is the disperion period (Beltaos, 1980).

4.8 Half-Life of Dye Mass Tracer

The total dye mass calculated for each sampling time gives a time record of the amount of tracer remaining in the estuary. The total dye mass for each time step is calculated by:

$$M_s = \int_{-\infty}^{\infty} C'(X,t)\, dX \qquad (28)$$

The half-life of the dye tracer is a measure of the flushing time of the estuary (Blair, 1976). The half-lives were calculated by the following equations:

$$T_{50} = T_0\ (M_s) - T\ (0.5\ M_s) \qquad (29)$$

where

T_{50} = Half-life of dye tracer

$T(M_s)$ = Time at which mass equals M_s

$T(0.5M_s)$ = Time at which total dye mass is reduced by one-half to $0.5\ M_s$

4.9 Half-life of the Maximum Dye Concentration

The half-life of the maximum dye concentration was found by Blair (1976) and Fisackerly (1974) to be an indicator of the longitudinal distribution of dye tracer in the estuary. The half-life of the maximum dye concentration is found by:

$$\tau_{50} = \tau_0 \ (C_{max}) - \tau \ (0.5 \ C_{max}) \tag{30}$$

where

τ_{50} = Half-life of maximum concentration

$\tau_0 \ (C_{max})$ = Time of maximum concentration

$\tau_0 \ (0.5 \ C_{max})$ = Time to reduce maximum concentration by one-half to $0.5 \ C_{max}$

An advantage of using this method and the half-life of the dye mass is that they involve the spreading of the tracer in all 3-dimensions, therefore,eliminating the assumptions needed for using a one-dimensional analysis.

CHAPTER 5.

RESULTS AND DISCUSSIONS

5.1 Model Fresh Water Discharge and Salinity

The fresh water discharge values into the north and south branch of the Lafayette River are listed in Table 3. Run B had the lowest discharge rate into the Model, with the flow into the north branch 6.4% greater than the south branch. The discharge rate for Run C was 3.74 times faster than the flow of Run B. Run C had the most variation in discharge rate, with the south branch flow 33.1% greater than the north branch. Run D was the highest discharge test performed with a flow rate 2.3 times faster than Run C and 8.4 times faster than Run B. The flow into the north branch was faster than the south branch by 3.9%. The inconsistent flow into the branches for all three tests was due to the difficulty in calibrating each Roto-meter to the same flow rate. This inconsistency will probably effect any analysis in the branches of the river, but should not affect the data for the main channel. Run A was a continuous dye release test not used for the present study.

The total fresh water discharge value for Run B, when scaled up to the prototype equivalent of 0.919 m^3/sec (32.47 ft^3/sec) is very close to the estimated mean river discharge calculated from annual rainfall data by White (1972) of 0.89 m^3/sec (31.60 ft^3/sec). This indicates that the discharge rate for Run B simulated the normal prototype conditions found by White (1972).

Observations of the salinity field in the Lafayette River reveal a small gradient in the main branch of the River for all three tests. Figure 7 shows that the mean salinity gradient, based on the average

TABLE 3. FRESH WATER DISCHARGE Q_f

IN M^3/SEC ($\times 10^{-6}$) ($(FT^3/SEC)(\times 10^{-4})$)

EVENT	NORTH BRANCH		SOUTH BRANCH		RIVER TOTAL	
RUN B	0.474	(0.167)	0.445	(0.157)	0.919	(0.325)
RUN C	1.476	(0.521)	1.965	(0.694)	3.440	(1.215)
RUN D	3.947	(1.394)	3.797	(1.341)	7.744	(2.735)

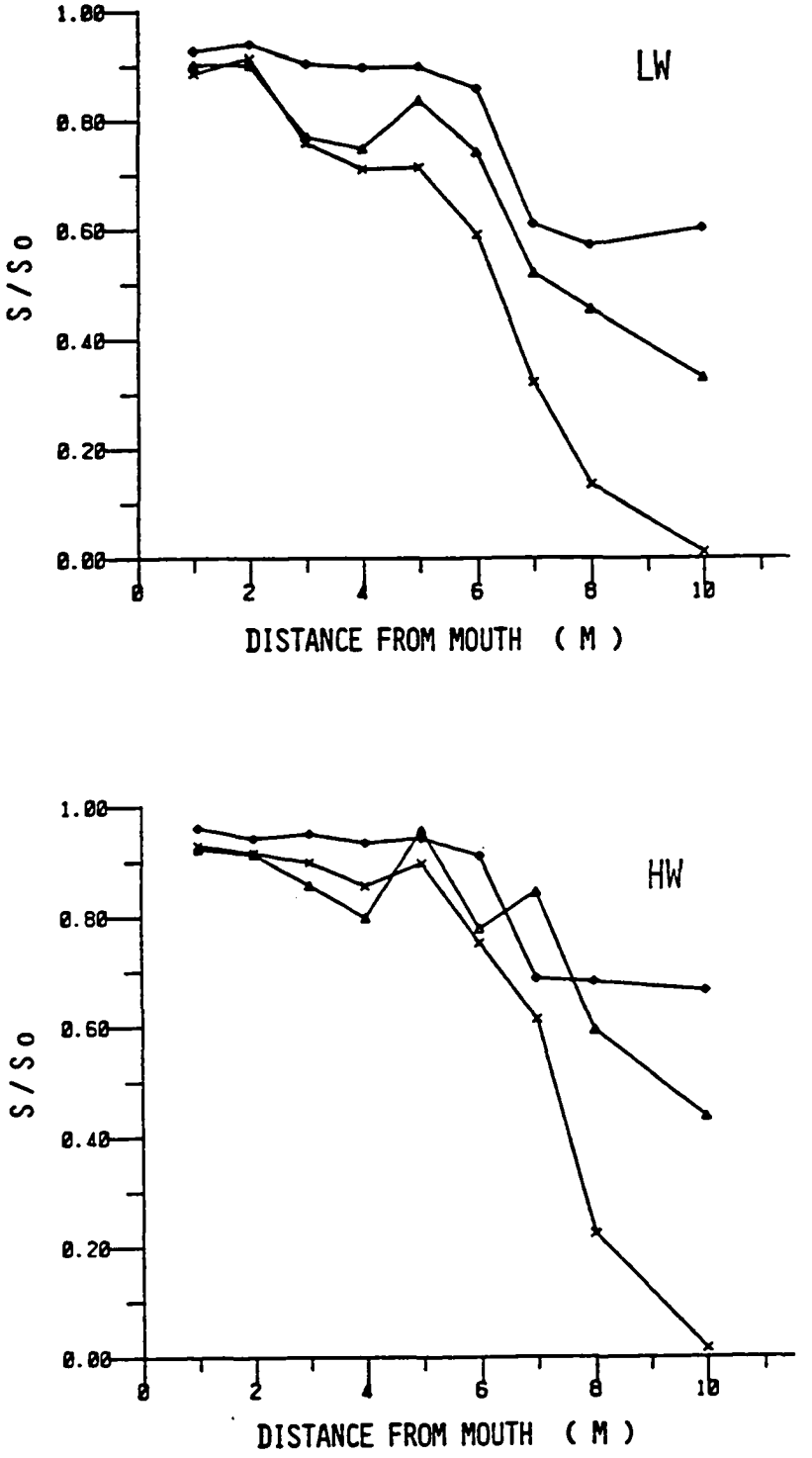

Figure 7. Mean Horizontal Salinity Profiles for the Main Channel and North Branch Stations (◇ = Run B, Δ = Run C, and X = Run D)

salinity over all sets of samples for each run, increased with fresh water discharge.

The effect of the increase in fresh water discharge into the River can best be observed by looking at the vertical salinity profile. Figure 8 displays the surface and bottom salinity values for the central deep station sampled (L4). As the discharge rate increased from Run B to Run D, the River switched from being essentially vertically homogeneous (1 ppt change from top to bottom) to a stratified condition (4 ppt change).

The estuary numbers calculated from equation (5) for all three tests with normal, above normal, and heavy fresh water discharge conditions were 145.51, 39.03, and 17.46 respectively. Thus according to Pritchard's (1967) definition of the estuary number the classification of the River switched from well-mixed for the low flow test, to partially mixed for the high discharge test.

5.2 Estuarine Richardson Number

Fischer (1972) defined the Estuarine Richardson Number as the input of buoyancy per unit width due to the river flow. The Number is a measure of the degree of stratification of an estuary. The values for all three tests from equation (6) yield the following results:

Test	$R_{IE}(X10^{-3})$
Run B	1.826
Run C	12.190
Run D	20.350

They indicate that as the fresh water discharge increased, the value of R_{IE} also increased. The values are well below the transition

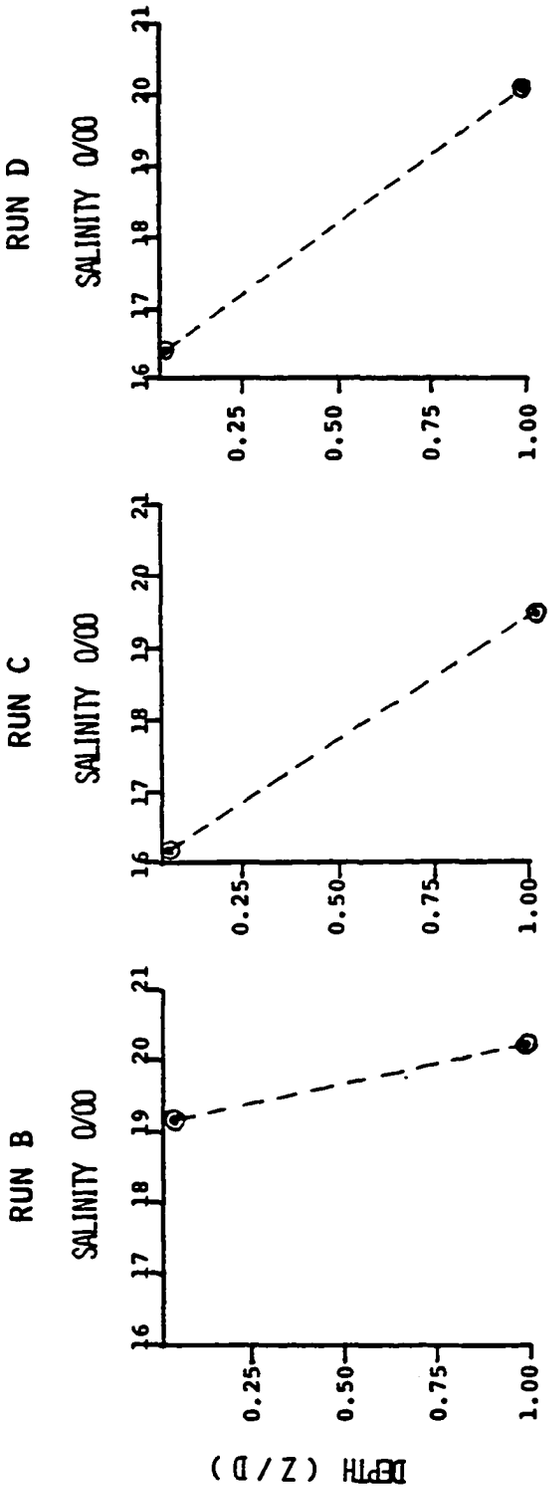

Figure 8. Surface and Bottom Salinity Data from Station L 4

region of $0.08<R_{IE}>0.8$ stating that the model experiments increased in stratification, but did not reach a highly stratified condition. This result agrees with the vertical salinity profiles and the estuary number classification.

5.3 Hansen - Rattray Classification Model

A third test for estuary classification applied was the Hansen-Rattray Model which is based on the parameters of estuary circulation and stratification. Due to the fact that the Lafayette River branches at station L7, the Hansen-Rattray Model was run for the main channel (stations L1-L7) and the main channel with the north branch stations (stations L1-L10n) (see Table 4).

For the main channel, stations L1-L7, the values of the Froude Number increased from Run B to Run D indicating an increase in stratification. The value of β, the gradient parameter, decreased with fresh water flow, also indicating that stratification increased and gravitational convection became more important. The fact that β for Run C is larger than Run B is probably due to the inconsistent fresh water flow of the Run. The βRa term indicates that there is a flow reversal at depth for all three tests. As the fresh water discharge increased, M/β the tidal mixing parameter decreased, P increased, Ra decreased, and M decreased. Stations L1-L10n show similar results but are of higher stratification. The model is very shallow in River branches and due to bottom roughness features may give higher salinity readings.

From equation (8) the vertical salinity profiles can be calculated (Figure 9). The profiles generated from the Hansen-Rattray model (solid lines) indicate that the River increased in stratification as fresh water discharge increased. The Model is designed to predict the

TABLE 4. HANSEN-RATTRAY CLASSIFICATION MODEL FOR THE MAIN CHANNEL (STATIONS L1-L7) AND MAIN CHANNEL WITH NORTH BRANCH (STATIONS L1-L10)

STATIONS L1-L7

EVENT	Fm	$\frac{1}{\rho}$	β	$\frac{\partial S}{S_0}$	βRa	M/β	Ra	M
RUN B	4.27×10^{-3}	198.03	0.8424	0.0373	958.0941	82.1081	1137.2891	69.1709
RUN C	1.79×10^{-2}	52.92	0.8674	0.0846	325.8378	12.9435	375.6326	11.2277
RUN D	2.93×10^{-2}	23.51	0.7832	0.1819	226.1013	4.1569	288.7029	3.2552

STATIONS L1-L10n

EVENT	Fm	$\frac{1}{\rho}$	β	$\frac{\partial S}{S_0}$	βRa	M/β	Ra	M
RUN B	4.15×10^{-3}	198.03	0.8357	0.0381	979.2597	82.1083	1171.8442	68.6144
RUN C	1.19×10^{-2}	52.92	0.7656	0.1107	445.2967	12.9435	581.6437	9.9093
RUN D	2.05×10^{-2}	23.51	0.6533	0.2240	295.5572	4.1565	452.3967	2.7155

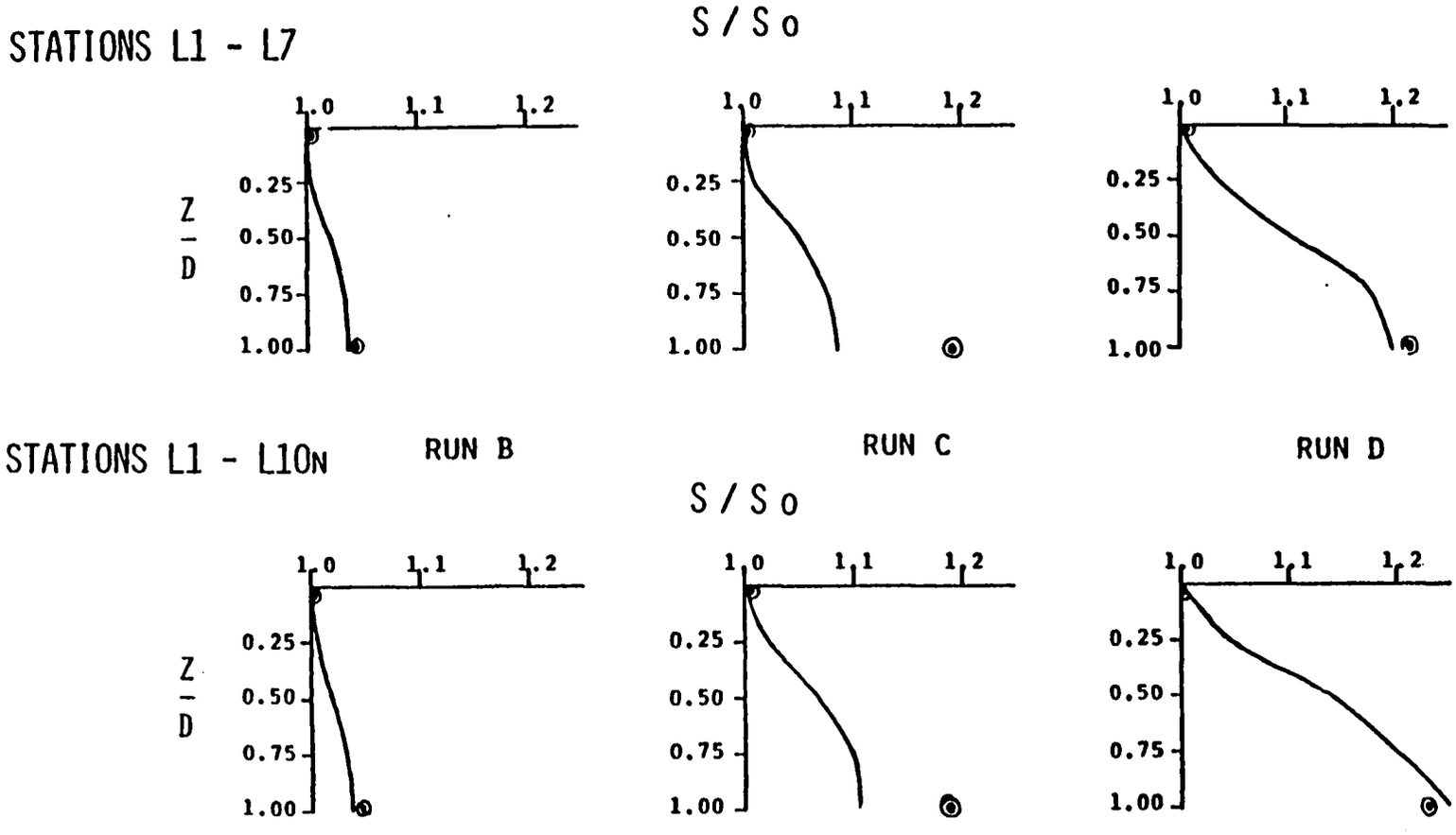

Figure 9. Vertical Salinity Profiles Predicted from the Hansen-Rattray Model (Solid Line)for both Approaches. Single Points are Surface and Bottom Data from Station L 4.

conditions at a central portion of the River, therefore,data collected from station L4 was superimposed on the vertical salinity profiles. The correlation for both approaches, using the main channel with north branch stations, yields good results, therefore,verifying the results of the vertical salinity profiles predicted from the Hansen-Rattray classification model.

Since the salinity profiles correlate so well between the collected data and the values predicted by the Model, it is reasonable to accept that the horizontal velocity profiles (U/U_f) predicted by the model (equation 7) are credible, although no attempt was made to verify them. The velocity profiles (Figure 10) reveal a flow-reversal at depth for all three tests, and that the net flow towards the mouth of the River increases with fresh water discharge. White (1972) found similar results in a prototype study of the Lafayette River. Under normal fresh water discharge conditions, there was a slight flow-reversal at depth for stations near the mouth of the River. After heavy rainfall, the flow-reversal was more pronounced.

The model values calculated for the circulation parameter (U_s/U_f) and stratification parameter ($\partial S/S_0$) are plotted on the Hansen-Rattray stratification-circulation diagram (Figure 11). The results are as follows:

Run B is of type 2a which indicates that there is flow-reversal at depth with both advection and diffusion contributing to the upstream salt flux. The position also indicates that Run B is the least stratified of the three tests.

Run C has a split result, depending on which approach is taken, the main channel or the main channel with the north branch stations.

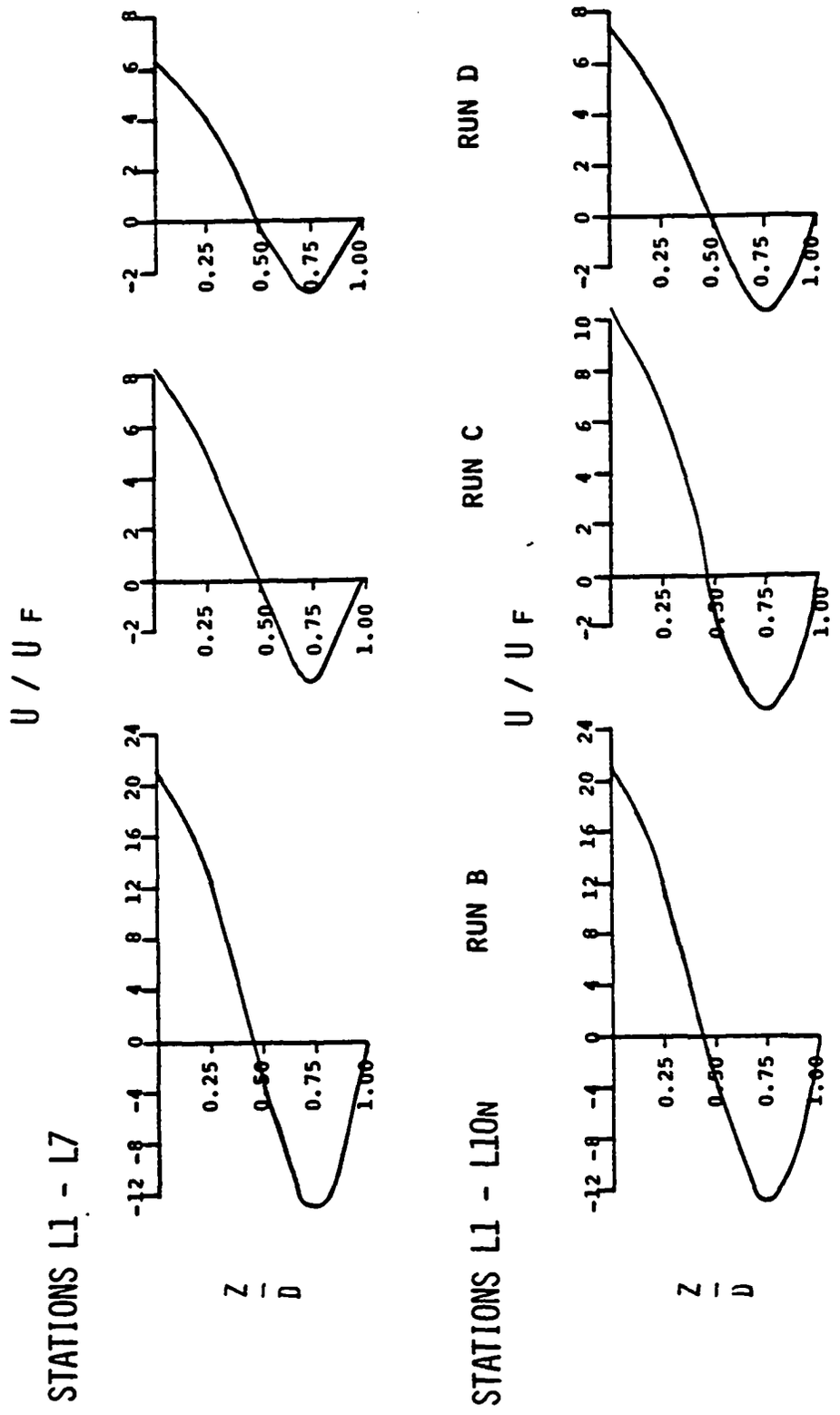

Figure 10. Velocity Profiles Predicted from the Hansen-Rattray Model for Both Approaches.

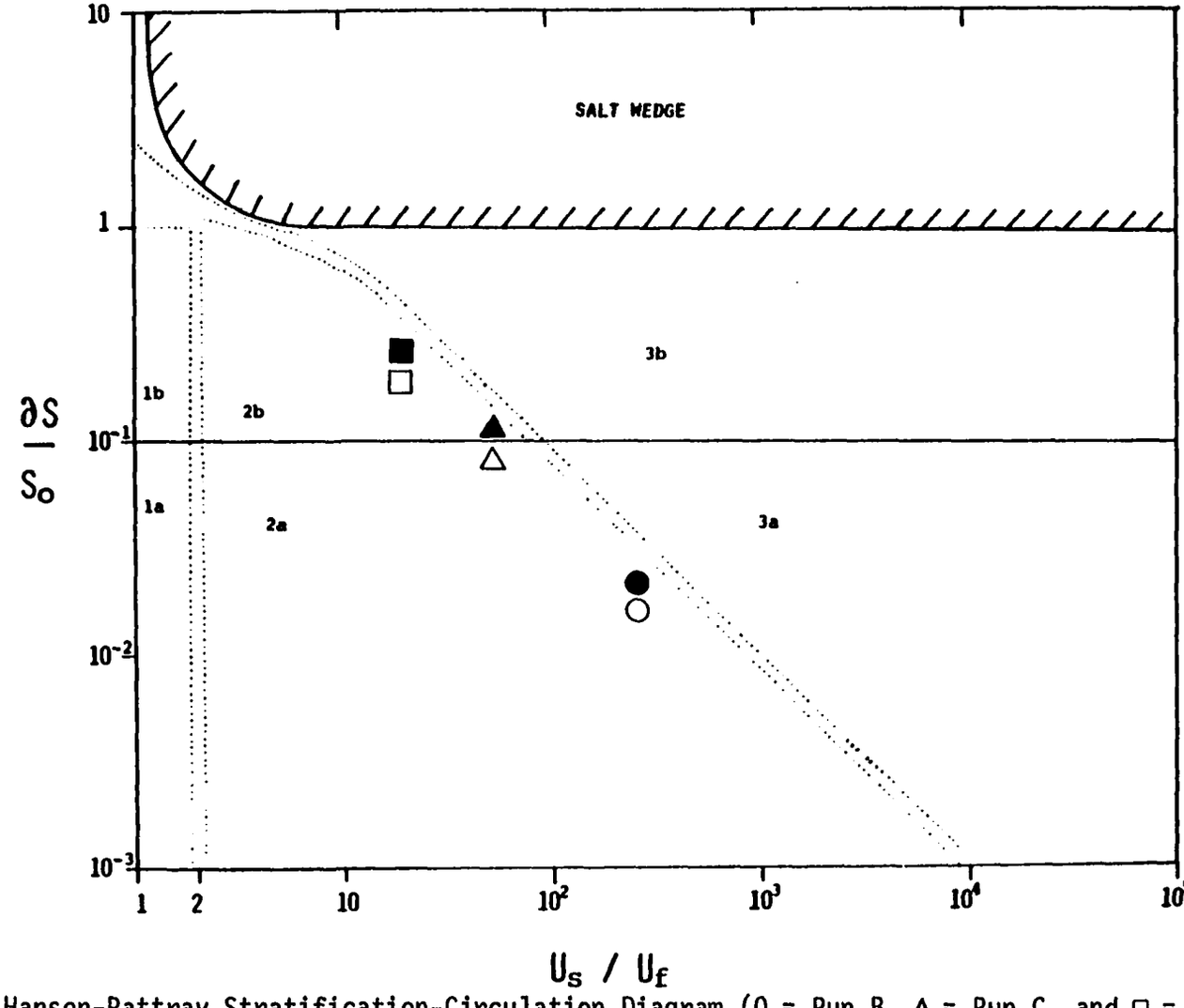

Figure 11. Hansen-Rattray Stratification-Circulation Diagram (O = Run B, Δ = Run C, and □ = Run D). Stations L1 and L7, Open Symbols; and Stations L1 - L10N, Closed Symbols.

The main channel (stations L1-L7) indicates a stronger stratification than Run B and falls in the upper region of type 2a. The main channel with the north branch stations (stations L1-L10n) is type 2b, which indicates the River is higher stratified than the main channel approach. Run C also had the largest variation in discharge rate into the model.

Run D is type 2b for both approaches, indicating stronger stratification. This fact puts the River system simulated by Run D in a different classification category than the other tests, showing that Run D crossed a threshold value of river discharge between Run C and Run D.

It is also apparent from Figure 11 that the Lafayette River could be looked at as two separate systems. From the two section approach station L1-L10n showed a stronger stratification than stations L1-L7. The fact that the branches are narrow, shallow, and close to the fresh water source could bias the results and should be treated as a separate system.

The results of the Hansen-Rattray Model appear good. From a few simple measurements it is possible to get a picture of the estuary classification along with the vertical and horizontal velocity profiles.

5.4 Tidal Trapping

One of the mechanisms used to explain mixing in an estuary is trapping. The term is used to describe the effects of side embayments and small branching channels on mixing. Fischer (1979) explains trapping as follows: The propagation of the tide represents a balance between the inertia of the water mass and the pressure force due to the slope of the water surface, i.e. the slope of the tidal wave. As an example, consider a dye release in a typical coastal plain estuary

(Figure 12) with one major channel and a number of side embayments. In the main channel the tidal elevations and velocities are not usually in phase, that is to say that high water occurs before high water slack and low water slack. This is caused by the momentum of the flow in the main channel, which causes the current to flow for a time against the pressure gradient. The side embayment with a lower current velocity has less momentum, and the current direction changes when the water level begins to drop. Figure 12-a shows the cloud of dye being carried upstream by the flood tide. Some dye enters the side embayment and some continues upstream in the main channel (Figure 12-b). The particles in the side channel now return to the main stream, but now lag the original dye cloud (Figure 12-c). This separation distance can be as much as the travel distance in the main channel between high water and slack water. On the ebb tide, the side channel discharge will lead the original dye cloud.

This effect can be seen in the Lafayette River by looking at the normalized dye concentration profiles versus high water tidal cycles for the embayment sampled (station L5.5) and its two adjacent stations (L5 and L6) (Figure 13a). With the dye released at LW 1, Run B shows that a high concentration of dye enters the embayment at HW 2 and very little recorded at the adjacent stations. At HW 4 there is less dye in the embayment and peaks observed at stations L5 and L6, showing that the dye is mixing and moving upstream (towards station L6). After HW 6 the cross-sectional mixing appears to be complete and the effect of trapping is not as obvious. Runs C and D show the same results with the net movement upstream (Figure 13 b and c).

Another effect of trapping can be seen by looking at the normalized

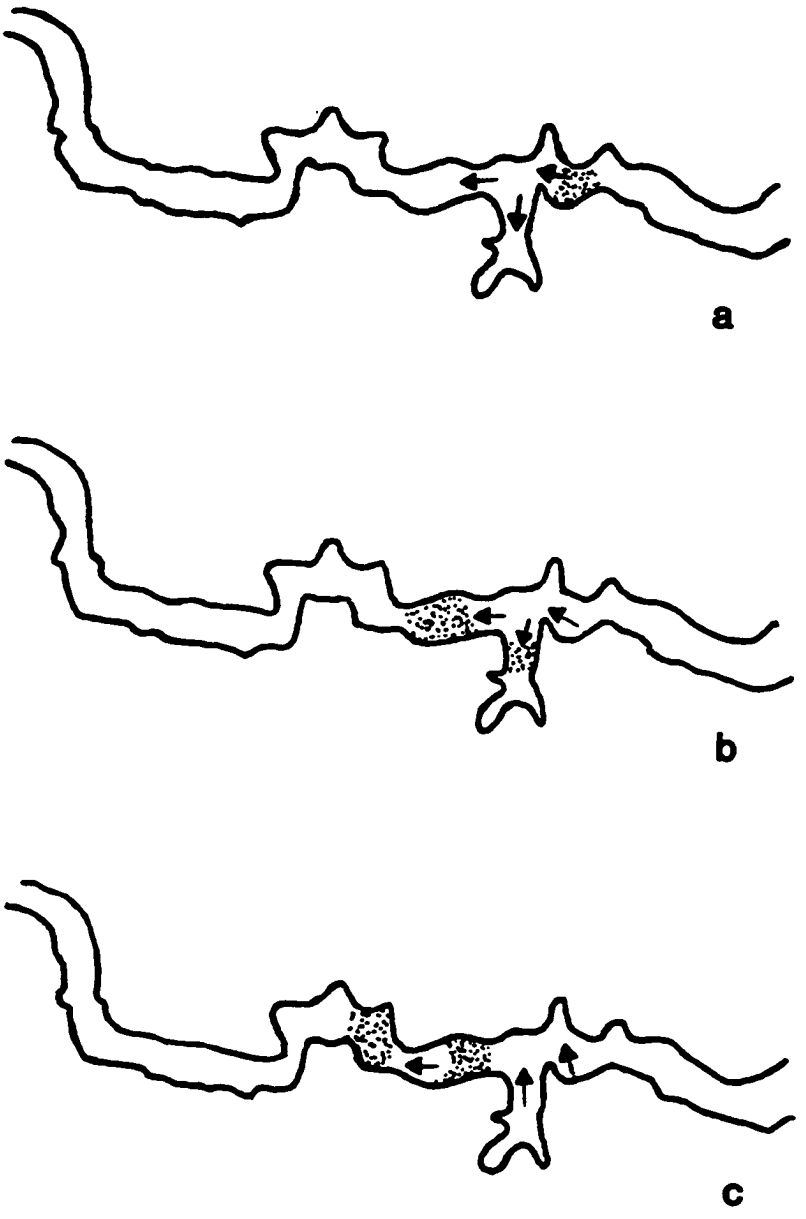

Figure 12. Coastal Plain Estuary with Side Embayments. Dots Represent a Dye Tracer Moving with the Flood Tide (Direction of Arrows) (after Fischer et al., 1979).

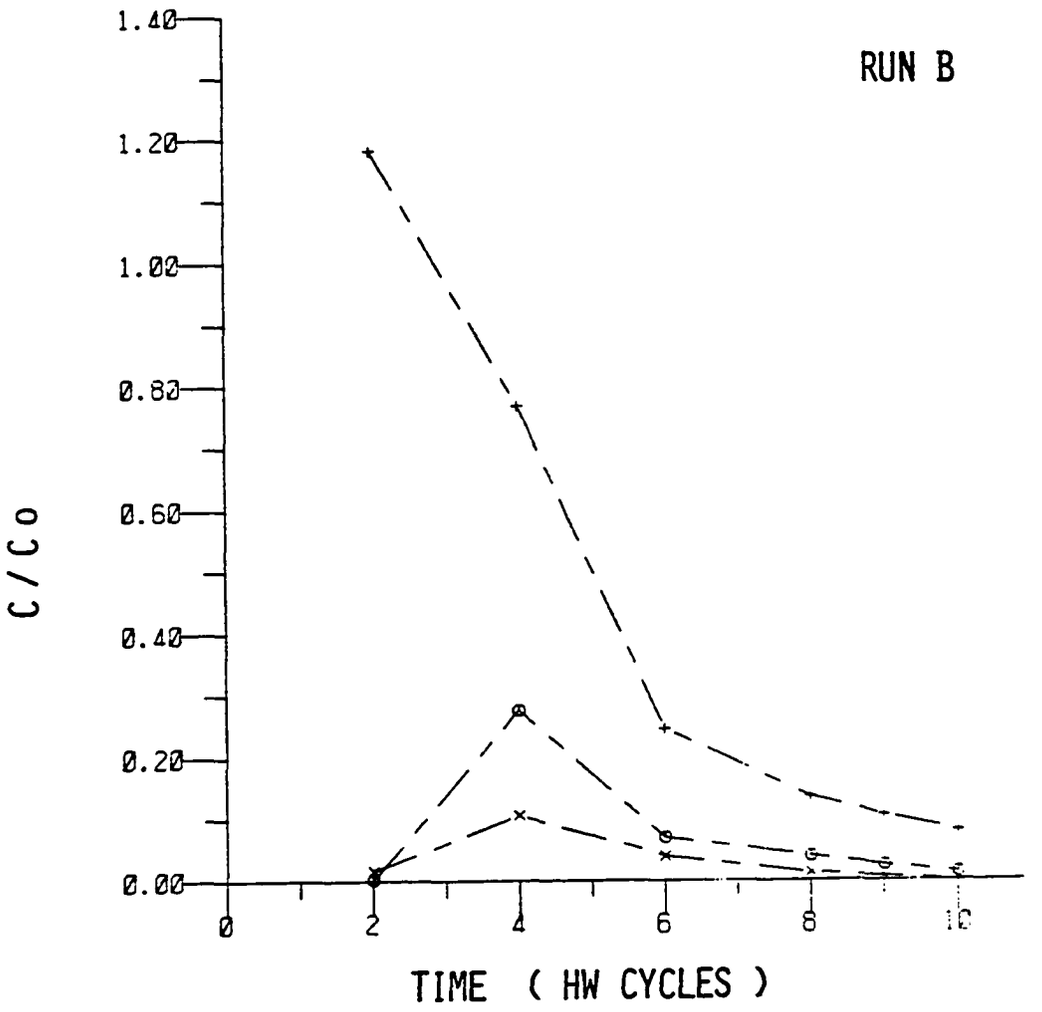

Figure 13a. Dye Concentration Versus High Water Tidal Cycles for Run B (X = Station L5, + = Station L5.5, and O = Station L6).

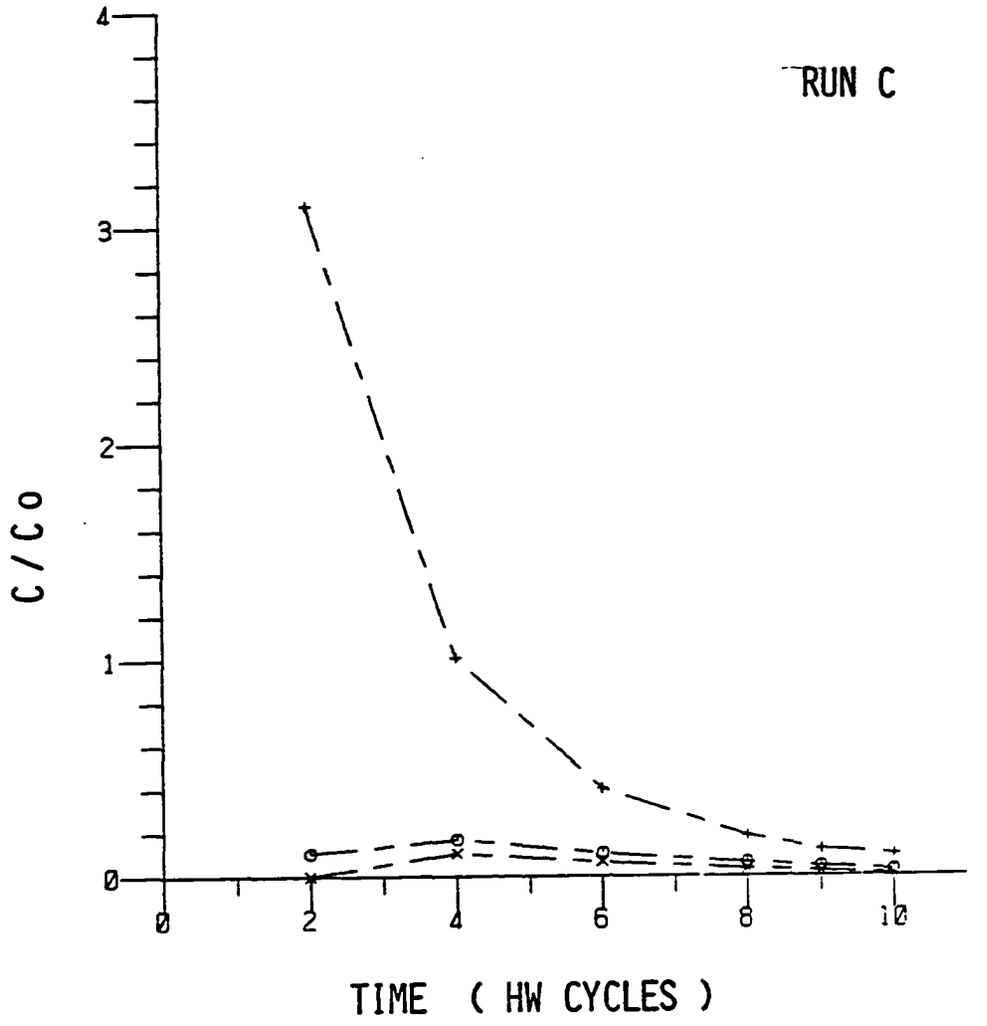

Figure 13b. Dye Concentration Versus High Water Tidal Cycles for Run C (X = Station L5, + = Station L5.5, and O = Station L6).

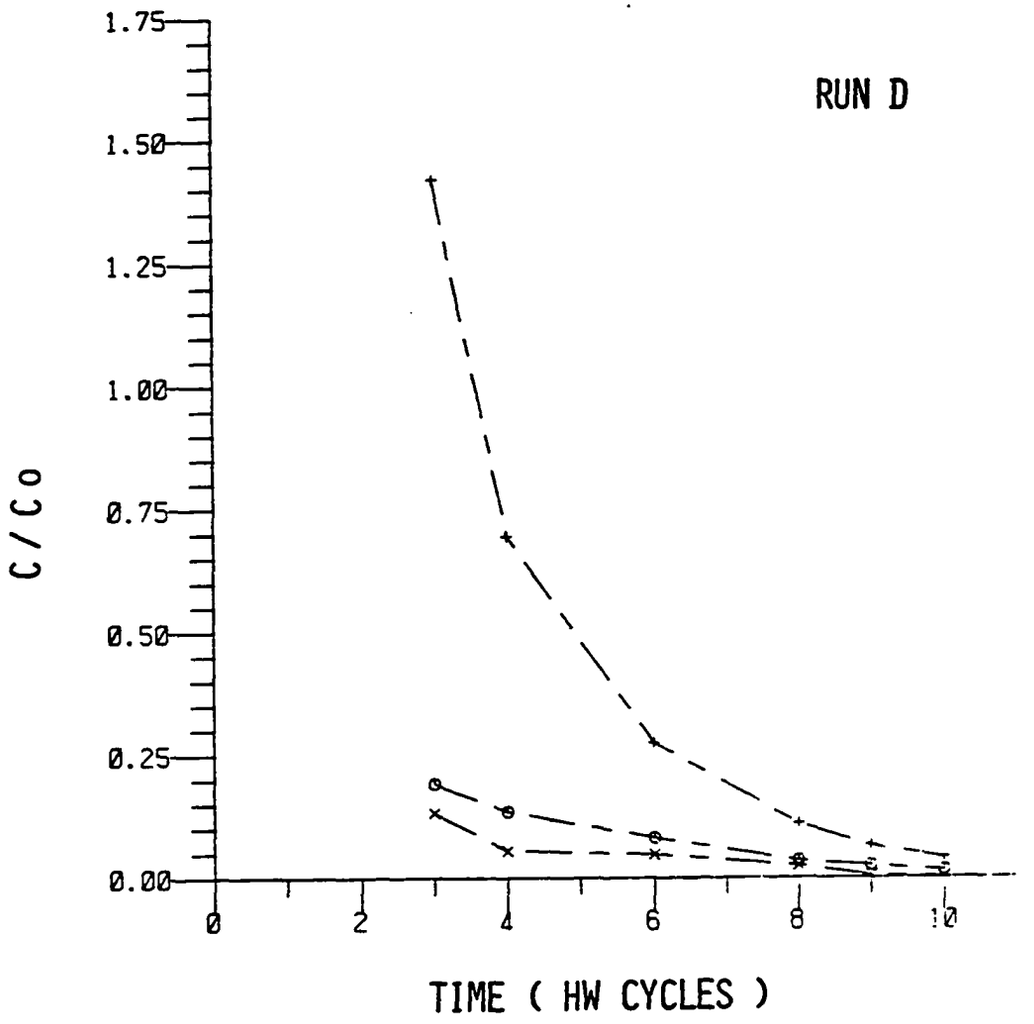

Figure 13c. Dye Concentration Versus High Water Tidal Cycles for Run C (X = Station L5, + = Station L5.5, and O = Station L6).

dye concentration profile versus distance for LW 4 (Figure 14 a, b, and c). The distribution is bimodal showing that the main dye cloud has separated. This separation occurs after station L5.5 with peaks at L4 and L8. Something resembling the effect of trapping occurs in most coastal plain estuaries and is an area that needs further study.

5.5 One - Dimensional Analysis

In order to apply a one-dimensional analysis, the estuary has to be long, narrow, and sufficiently unstratified. Since the Lafayette River is long and fairly unstratified, the width of the River caused a problem in the fact that it is not uniform in cross-section (see Table 5). The dye concentration data was transformed into an estuary of uniform cross-sectional area by using equation (14). The one-dimensional profiles (Figure 15 a, b, and c) still do not represent a normal "bell" shaped curve. They represent more of a bimodal distribution with the second peak at the beginning of the branches. This would indicate that the River is possibly 2 or 3 independent systems, the main channel being the major system and the north and south branches the minor systems. This conclusion agrees with the results of the Hansen-Rattray Model when it showed a change in the degree of stratification depending on whether the analysis considered stations L1-L7 or L1-L10n.

The branches of the River in the model are very shallow and narrow and the data could be influenced by the water surface tension effects. Due to this fact and with the lack of complete data from the branches, the remainder of the analysis will use data just from the main channel of the River.

5.6 Longitudinal Dispersion Coefficient by Salinity Intrusion

The longitudinal dispersion coefficient was found from equation

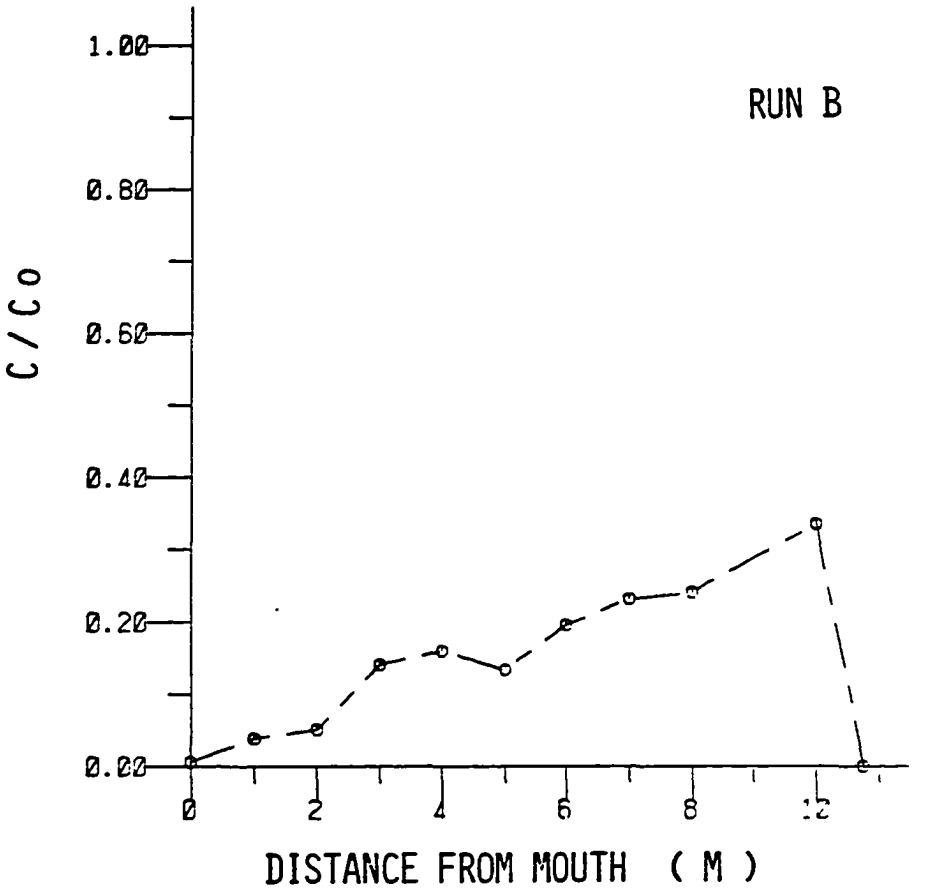

Figure 14a. Dye Concentration Versus Distance from the River Mouth for Run B. Sampling Event LW 4.

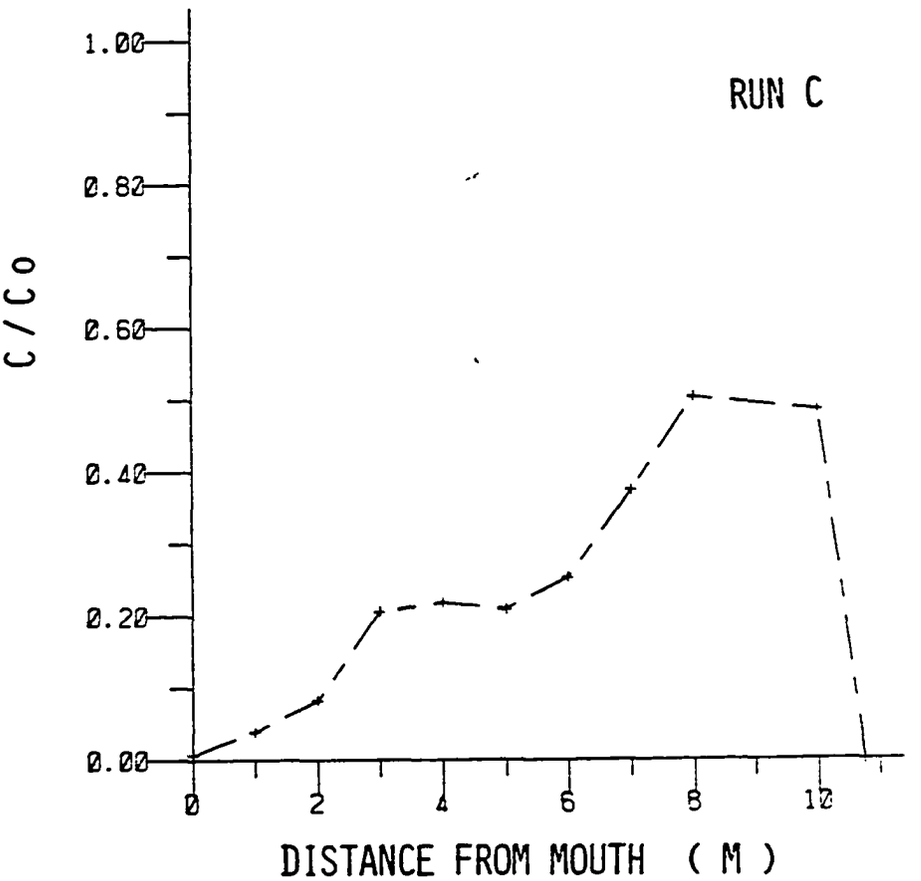

Figure 14b. Dye Concentration Versus Distance from the River Mouth for Run C. Sampling Event LW 4 .

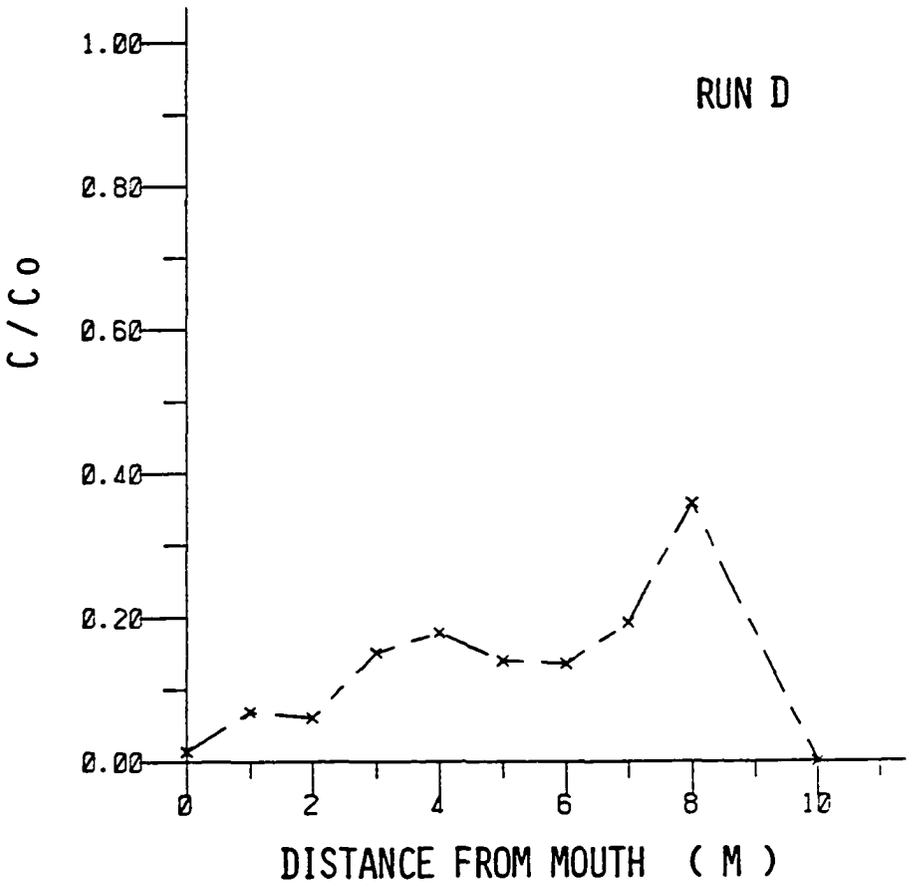

Figure 14c. Dye Concentration Versus Distance from the River Mouth for Run D. Sampling Event LW 4.

TABLE 5. CROSS - SECTIONAL AREA OF THE LAFAYETTE RIVER IN $M^2(ft^2)$

STATION	MEAN LOW WATER		MEAN HIGH WATER	
L1	0.00743	(0.0800)	0.01477	(0.1590)
L2	0.00808	(0.0870)	0.01449	(0.1560)
L3	0.00883	(0.095)	0.03378	(0.144)
L4	0.00753	(0.0810)	0.01179	(0.127)
L5	0.00585	(0.0630)	0.00971	(0.1045)
L6	0.00492	(0.053)	0.00845	(0.091)
L7	0.00378	(0.04071)	0.00683	(0.07351)
L8 S	0.00111	(0.012)	0.00251	(0.027)
L8 N	0.00195	(0.021)	0.00362	(0.039)
L10 N	0.00028	(0.003)	0.000929	(0.010)

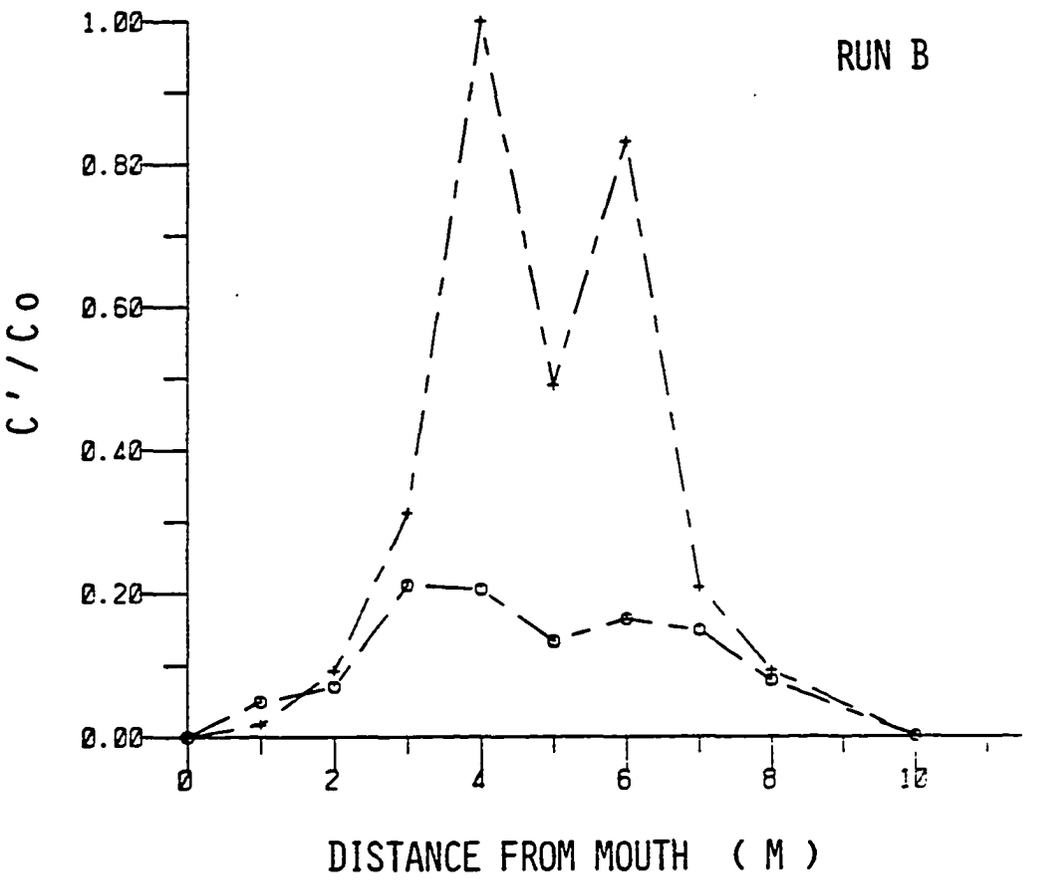

Figure 15a. C'/C_0 Versus Distance from the River Mouth for Run B (+ = LW2 and O = LW4).

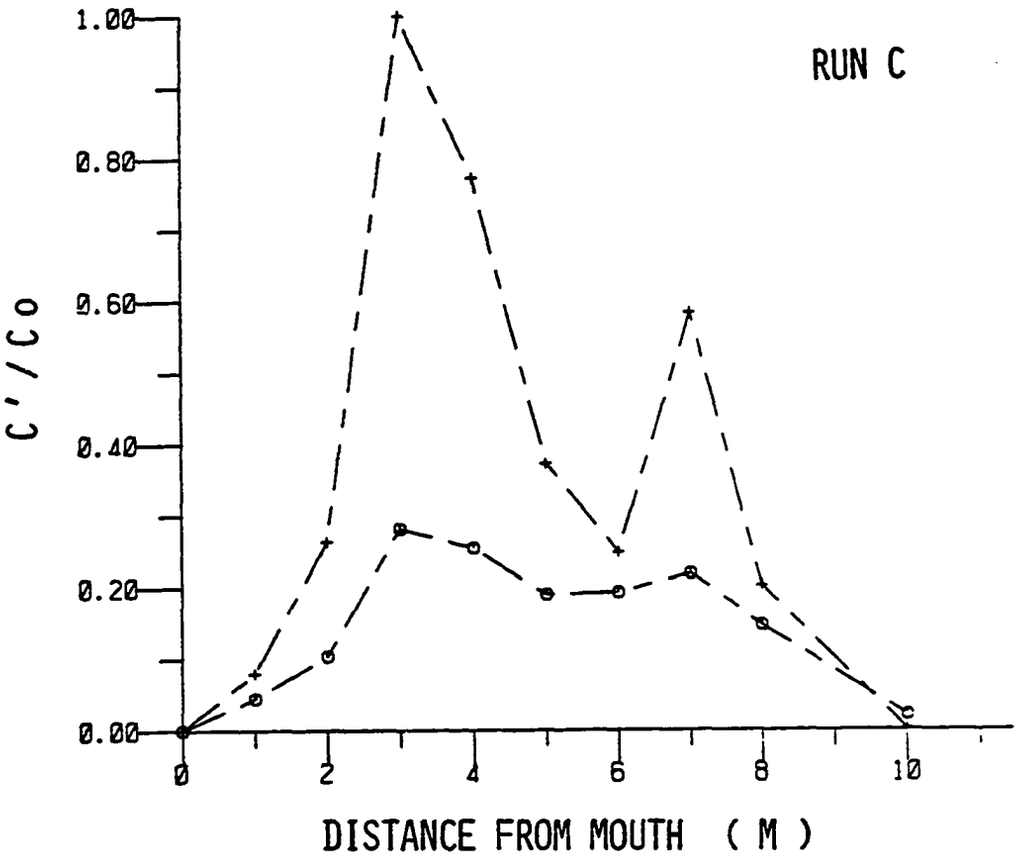

Figure 15b. C'/C_0 Versus Distance from the River Mouth for Run C (+ = LW2 and O = LW4).

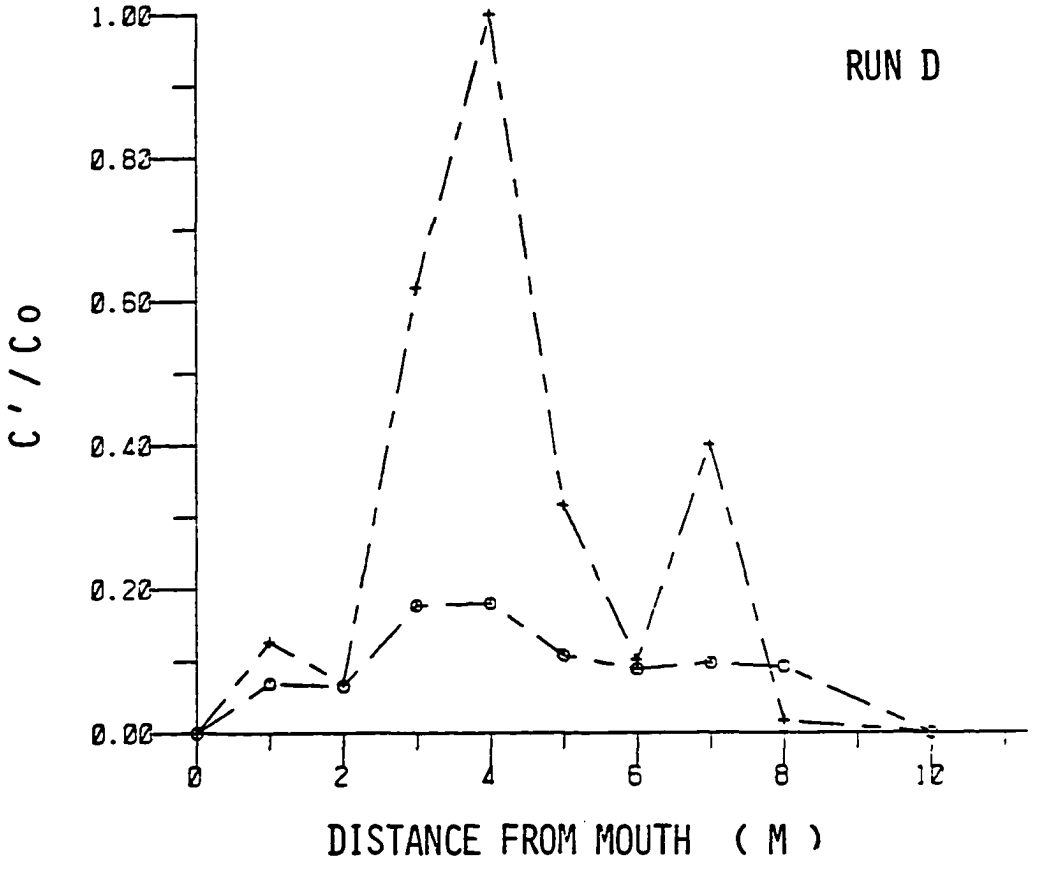

Figure 15c. C'/C_0 Versus Distance from the River Mouth for Run D (+ = LW2 and 0 = LW4).

(15) by using the longitudinal salinity gradient and corresponding fresh water flow. The salinity values for the main channel were used along with the cross-sectional areas in order to calculate the high and low water slack longitudinal dispersion coefficients. From Table 6, it can be seen that E is not constant for each Run. A possible reason for this is from fluctuations in the horizontal salinity profile, which could be the result of the inconsistent discharge rates of the Rotometers. There also appeared to be some irregularities in the profiles around station L3, where fresh water could have been trapped in the wider area of the River.

The plot of the average values of E versus fresh water discharge (Q_f) for the low water slack approximation show that E varied directly with Q_f (Figure 16). This result is not as obvious when looking at the high water slack approximation, because Run C shows a low value. This low value could be explained by the argument of flow irregularities. Therefore, the slack water approximation for the longitudinal dispersion coefficient appears to vary directly with fresh water discharge using the salinity data.

5.7 Longitudinal Disperson Coefficient by Dynamic Relationship

Thatcher and Harleman (1972) found a relationship showing that the local salinity gradient plus a term related to the geometry of the area approximates the longitudinal dispersion coefficient. Figure 17 shows the values from equation (17) for the high and low water slack approximations. The values calculated for the low water slack approximation vary directly with the increase with fresh water discharge. Except for Run C, the high water profile shows that the dispersion coefficient remained constant.

TABLE 6. LONGITUDINAL DISPERSION COEFFICIENT BY SALINITY INTRUSION METHOD, VALUES CALCULATED FOR STATIONS L1-L7

	RUN B		RUN C		RUN D	
SAMPLING TIME	M^2/sec	ft^2/sec	M^2/sec	ft^2/sec	M^2/sec	ft^2/sec
LW 2	0.0089	0.0953	0.0407	0.4381	0.0709	0.7634
LW 4	0.0070	0.0754	0.0061	0.0644	0.0207	0.2228
LW 6	0.0124	0.1336	0.0083	0.0890	0.0164	0.1763
LW 8	0.0073	0.0787	0.0049	0.0528	0.0115	0.1241
LW10	0.0122	0.1308	0.0048	0.0513	0.0117	0.1265
HW 2	0.0085	0.0919	0.0079	0.0847	0.0071 *	0.0767 *
HW 4	0.0064	0.0692	0.0048	0.0513	0.0630	0.6778
HW 6	0.0049	0.0523	0.0061	0.0653	0.0267	0.2867
HW 8	0.004	0.1014	0.0039	0.0419	0.0208	0.2276
HW 9	0.0038	0.0406	0.0056	0.00598	0.0234	0.2521
HW 10	0.0100	0.1072	0.0037	0.0401	0.0201	0.2164
MEAN LW	0.0096	0.1028	0.0129	0.1393	0.0262	0.2826
MEAN HW	0.0065	0.0649	0.0057	0.0608	0.0260	0.2801

* HW 3

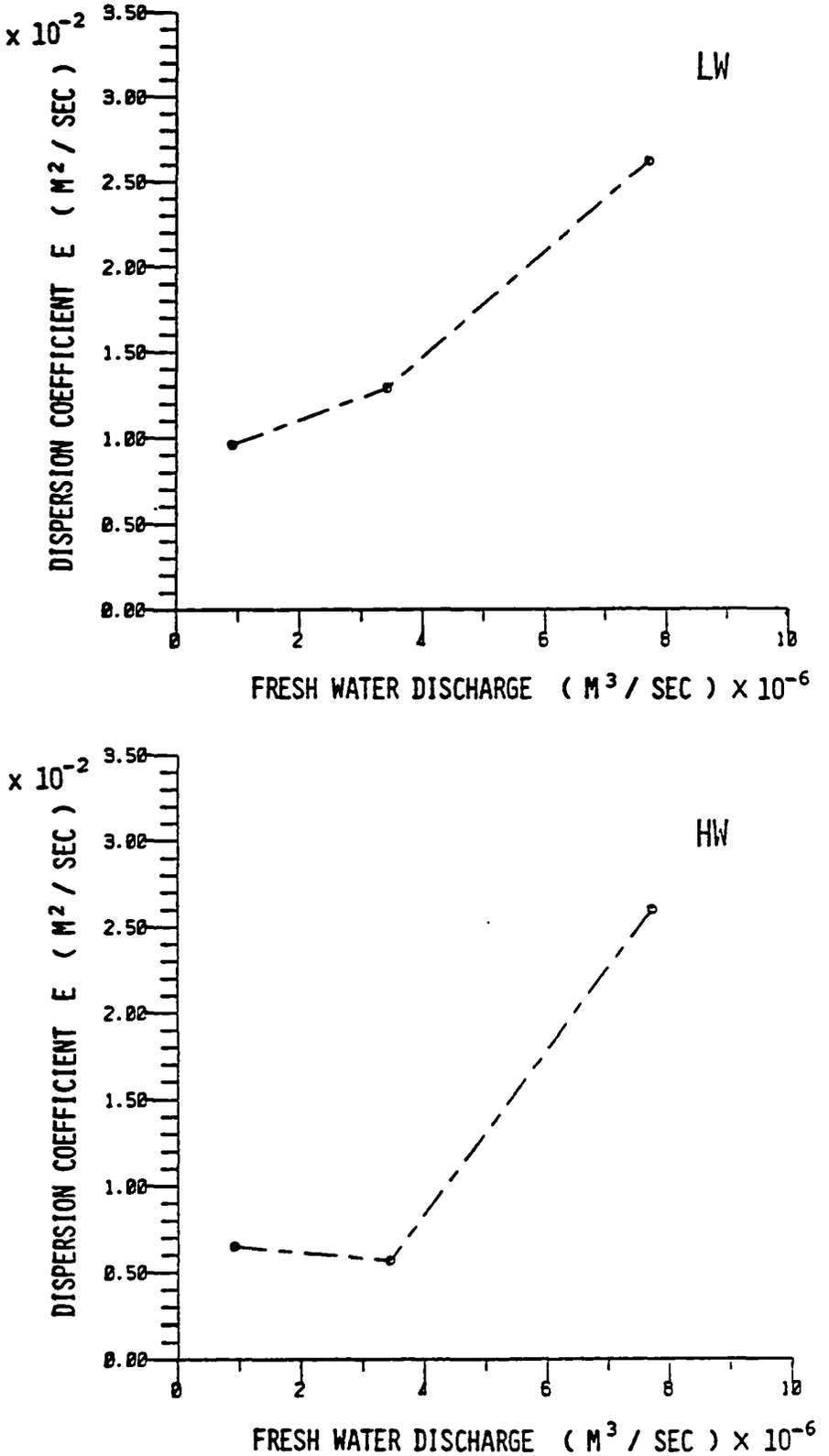

Figure 16. Slack Water Approximation for E Versus Fresh Water Discharge from the Salinity Intrusion Method.

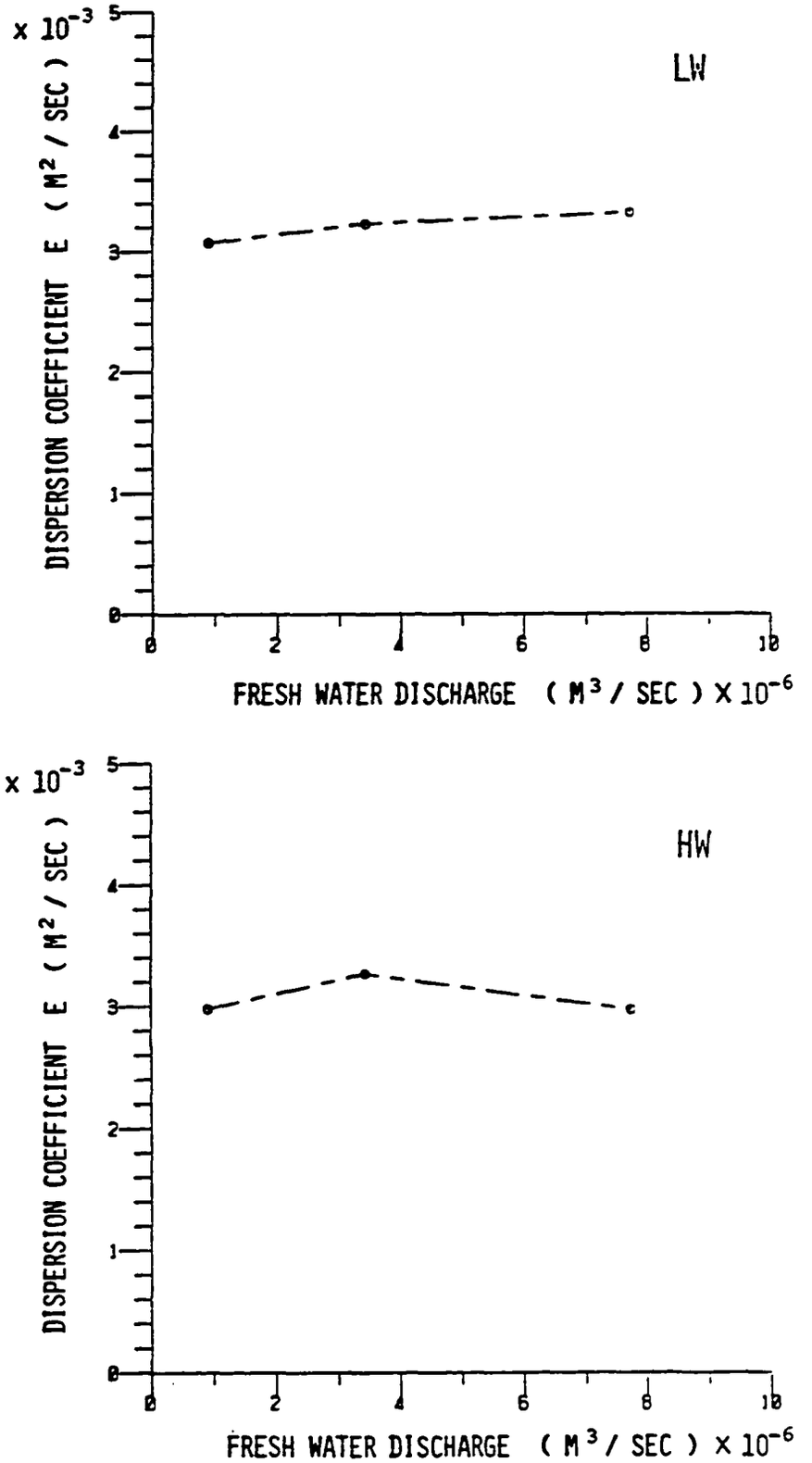

Figure 17. Slack Water Approximation for E Versus Fresh Water Discharge from the Dynamic Relationship Method.

The value of E_T calculated from equation (16) for all three tests is 2.3803 x $10^{-3}m^2$/sec (2.56 x $10^{-2}ft.^2$/sec). This term does not depend on fresh water discharge, therefore, it remains constant for all tests. The second term of equation (17) relates the effects of the salinity gradient on dispersion. The average values of K ($\partial S/\partial X$) for each run in m /sec are:

Test	LWS	HWS
Run B	$6.892X10^{-4}$	$5.981X10^{-4}$
Run C	$8.466X10^{-4}$	$8.857X10^{-4}$
Run D	$9.462X10^{-4}$	$5.948X10^{-4}$

Even though the K ($\partial S/\partial X$) term increased with discharge, it is still much smaller than the E_T term, therefore, E_T dominated E. It appears that the only time E can be dominated by K ($\partial S/\partial X$) is in a highly stratified estuary or if E_T is very small.

5.8 Longitudinal Dispersion Coefficient by the Change in Moment Method

The longitudinal dispersion coefficient was also calculated by the change in moment method using the one-dimensional dye concentration values (C') for the low and high water slack approximations. Table 7 displays the values for the various moments (from equations 20, 21, and 22), the mean of the distribution, and the variance. The dispersion coefficient was calculated for the sampling times that showed that the variance increased with time. The average dispersion coefficient values were plotted versus Q_f(Figure 18) from equation (26). The profiles did not increase with discharge but remained constant for the low water slack approximation. This can be explained by looking at the variance of each distribution. According to Taylor (1954) and Fischer (1979),

TABLE 7a. MOMENTS, MEAN, VARIANCE, AND LONGITUDINAL DISPERSION COEFFICIENT FOR RUN B FROM THE CHANGE IN MOMENT METHOD

EVENT	M_0	M_1	M_2	μ	σ^2	E
LW 2	.00238140	-.00106910	.00393290	-0.4141551	1.35202870	
						0.0003997
LW 4	.00078320	-.00081980	.00247620	-1.0467314	2.06599800	
						0.0000544
LW 6	.00041000	-.00045700	.00139640	-1.1146342	2.16344430	
LW 8	.00024940	-.00024840	.00077200	-0.9959904	2.10343220	
LW 10	.00012939	-.00011293	.00030983	-0.8727877	1.63278530	
HW 2	.00002842	.00000302	.00000302	0.1062632	.09497133	
						0.0007823
HW 4	.00094092	-.00021168	.00143992	-0.2249713	1.47971990	
						0.000316
HW 6	.00032059	-.00020516	.00078664	-0.6399451	2.04419620	
						0.0004441
HW 8	.00017770	-.00017290	.00067370	-0.9729882	2.84451510	
HW 9	.00006179	-.00000065	.00012472	-0.0105186	2.01817560	
HW 10	.00002164	.00000708	.00005076	0.3271719	2.23861480	

TABLE 7b. MOMENTS, MEAN, VARIANCE, AND LONGITUDINAL DISPERSION COEFFICIENT FOR RUN C FROM THE CHANGE IN MOMENT METHOD

EVENT	M_0	M_1	M_2	μ	σ^2	E
LW 2	.00198930	-.00264120	.00630680	-1.3277032	1.40756560	0.0002923
LW 4	.00077650	-.00081330	.00235110	-1.0473921	1.03078680	
LW 6	.00046480	-.00047540	.00144260	-1.0228055	2.05756940	
LW 8	.00026820	-.00028130	.00085110	-1.0488442	2.07330410	0.0000346
LW 10	.00015160	-.00017540	.00052200	-1.1569921	2.10464110	
HW 2	.00010100	.00010100	.00010100	1.0000000	.0000000	
HW 4	.00082510	-.00077690	.00225710	-0.9415828	1.84896900	0.0002575
HW 6	.00042320	-.00039640	.00135000	-0.9366730	2.31262490	0.0001371
HW 8	.00024470	-.00025040	.00088200	-1.0232938	2.55728330	
HW 9	.00014740	-.00011900	.00044780	-0.8073270	2.38621490	
HW 10	.00007417	-.00005848	.00022712	-0.7884589	2.44048700	

TABLE 7c. MOMENTS, MEAN, VARIANCE, AND LONGITUDINAL DISPERSION COEFFICIENT FOR RUN D FROM THE CHANGE IN MOMENT METHOD

EVENT	M_0	M_1	M_2	μ	σ^2	E
LW 2	.00161980	-.00206840	.00452320	-1.2769478	1.16184790	
						0.0005294
LW 4	.00049820	-.00066330	.00193150	-1.3313930	2.10434970	
						0.0000418
LW 6	.00027160	-.00036750	.00108870	-1.3530928	2.17760820	
LW 8	.00010480	-.00013068	.00035436	-1.2469466	1.82642200	
						0.0000917
LW 10	.00004799	-.00008110	.00023238	-1.6899354	1.98637720	
HW 3	.00260310	-.00337630	.00773090	-1.2970305	1.28759400	
HW 4	.00040010	-.00025720	.00085540	-0.6428393	1.72472310	
						0.0004098
HW 6	.00030950	-.00033610	.00112610	-1.0859451	2.45917240	
						0.0001148
HW 8	.00012430	-.00012530	.00045750	-1.0080451	2.66445660	
						0.0005298
HW 9	.00007310	-.00009086	.00034272	-1.2429549	3.14343530	
						0.0002075
HW 10	.00003457	-.00004019	.00016165	-1.1625687	3.32445370	

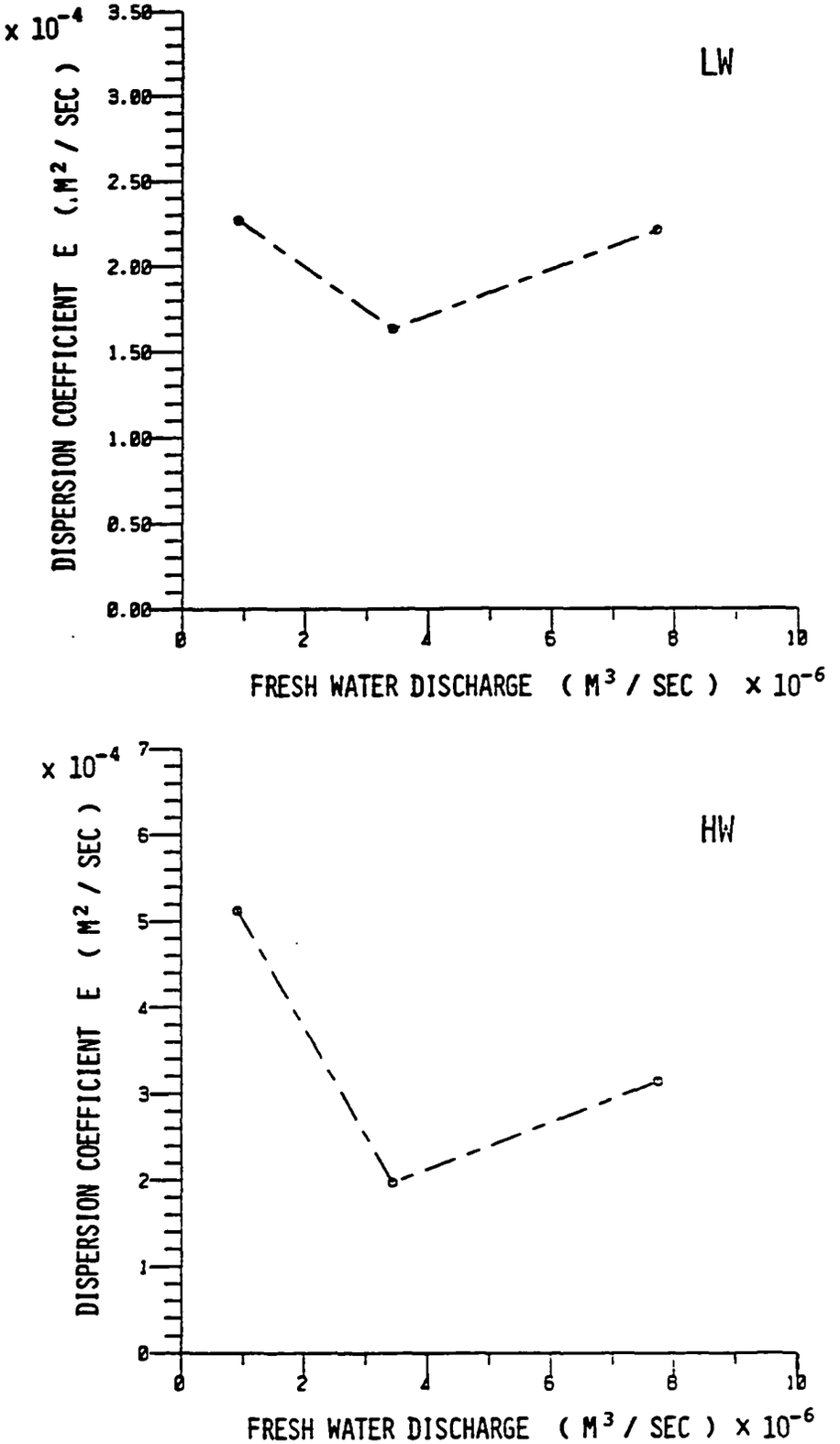

Figure 18. Slack Water Approximation for E Versus Fresh Water Discharge from the Change in Moment Method.

the variance of a distribution should increase with time as the dye becomes mixed with the water, but the variance calculated from the dye releases showed irregular results. The experiment was too short to calculate values of the variance into the dispersive period, but did show some increase with time. As stated previously, transverse mixing was assumed complete after HW 6. This agrees with the time of five tidal cycles found by Holley et al., (1970). It appears that the Lafayette River does not behave as a one-dimensional system for the dye distributions, even though the data was forced into a one-dimensional format for the short sampling period.

The values calculated for the mean μ indicate the position of the center of the dye mass. The values in Table 7 for μ show the distance away from the release point of the dye. The negative values indicate that the dye has moved toward the mouth of the River and positive values move toward the head. Figure 19 shows that as the fresh water discharge increased, the center of dye mass moved towards the mouth of the River.

5.9 Comparison of the Magnitude of E

The results of the three methods to calculate the longitudinal dispersion coefficient span two orders of magnitude. Using the model-to-prototype relationship for similitude, all of the values calculated fit into the range of the prototype values listed in Fischer (1979, Table 7.2). Each approach used a different computational model emphasizing different mixing processes. Each process neglects certain mechanisms (such as vertical mixing), which may in fact have been significant. Fischer (1979) suggests that errors of 100% are not unusual in mixing calculations. The two order of magnitude differences obtained

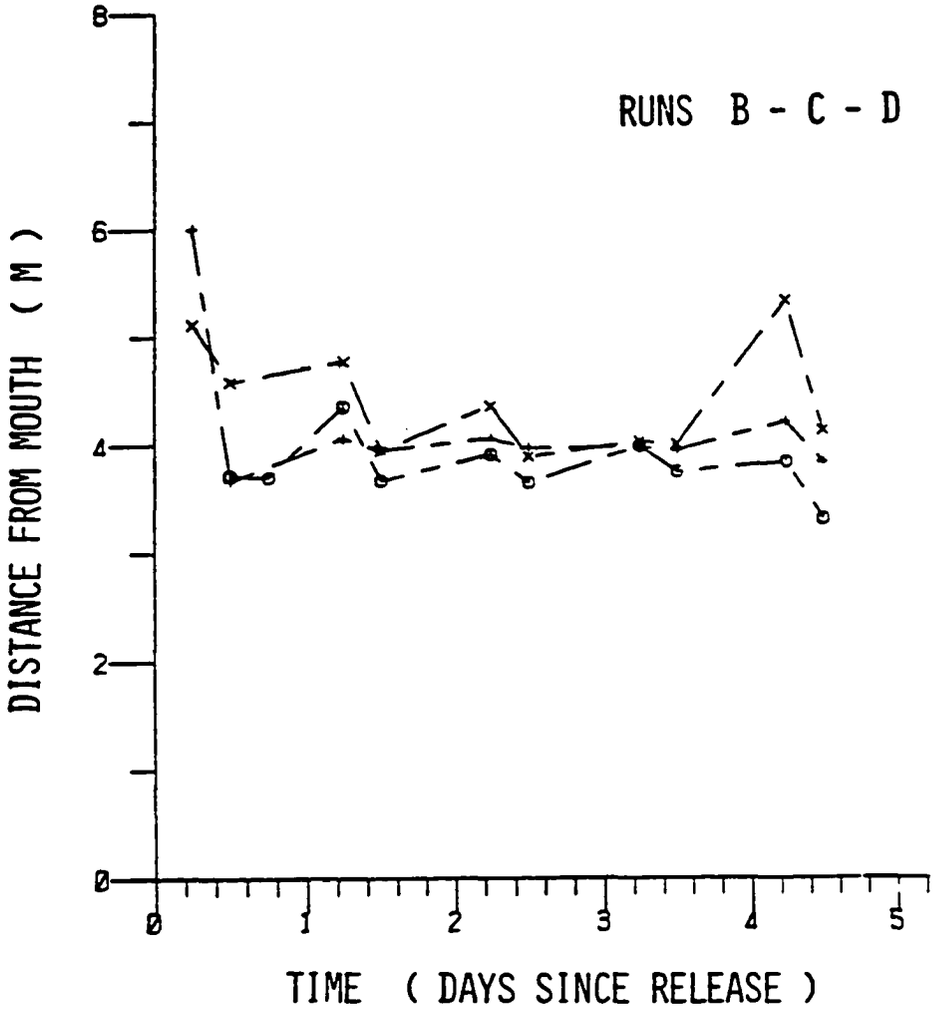

Figure 19. Position of the Center of Dye Mass Versus Time in Prototype Equivalent Days since Release.
(X = Run B, + = Run C, and O = Run D).

for E in this project are far beyond Fischer's limit. The reasons for this spread are not evident, however, and show the need for deeper investigation.

5.10 Half-life of Dye Mass Tracer

The total dye mass in the system for each Run versus time is plotted in Figure 20 a, b, and c. The fluctuations between the mass at high and low tides is small. This fluctuation is expected since some dye leaves the River mouth on the ebb tide and is carried back in on the flood tide.

After release of the dye at station L5, the time required to reduce the total dye tracer is an indicator of the flushing time of the river. The half-lives calculated from equation (29) are as follows:

Test	Time (Equivalent Prototype Days)
Run B	1.85
Run C	1.91
Run D	1.33

The results from this test shows that there is little difference between Run B and Run C, but Run D which had the highest fresh water discharge, had the fastest flushing rate.

5.11 Half-life of the Maximum Dye Concentration

The maximum concentration of dye tracer for each sampling time is given in Figure 21 a, b, and c. The half-life of the maximum dye concentration found from equation (30) yields the following results:

Test	Time (Equivalent Prototype Days)
Run B	1.05
Run C	1.09
Run D	0.57

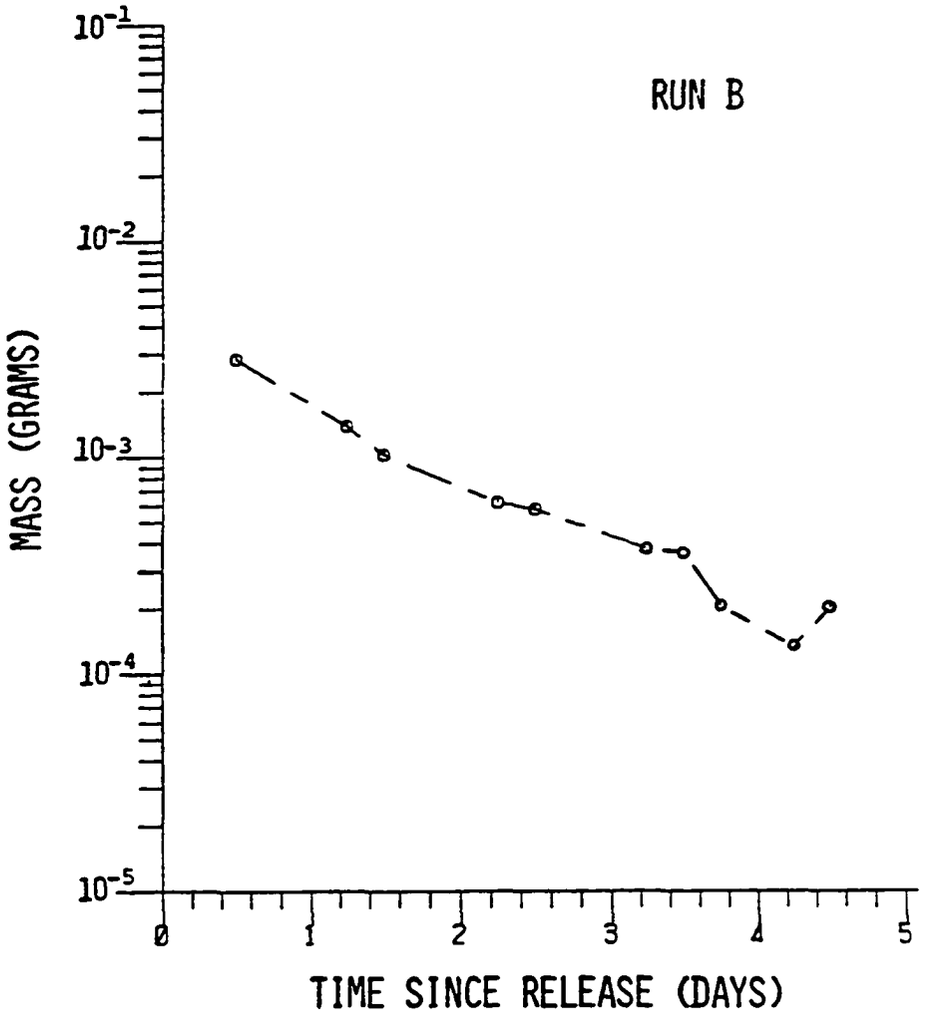

Figure 20a. Total Dye Mass in the River Versus Time in Prototype Equivalent Days since Release for Run B.

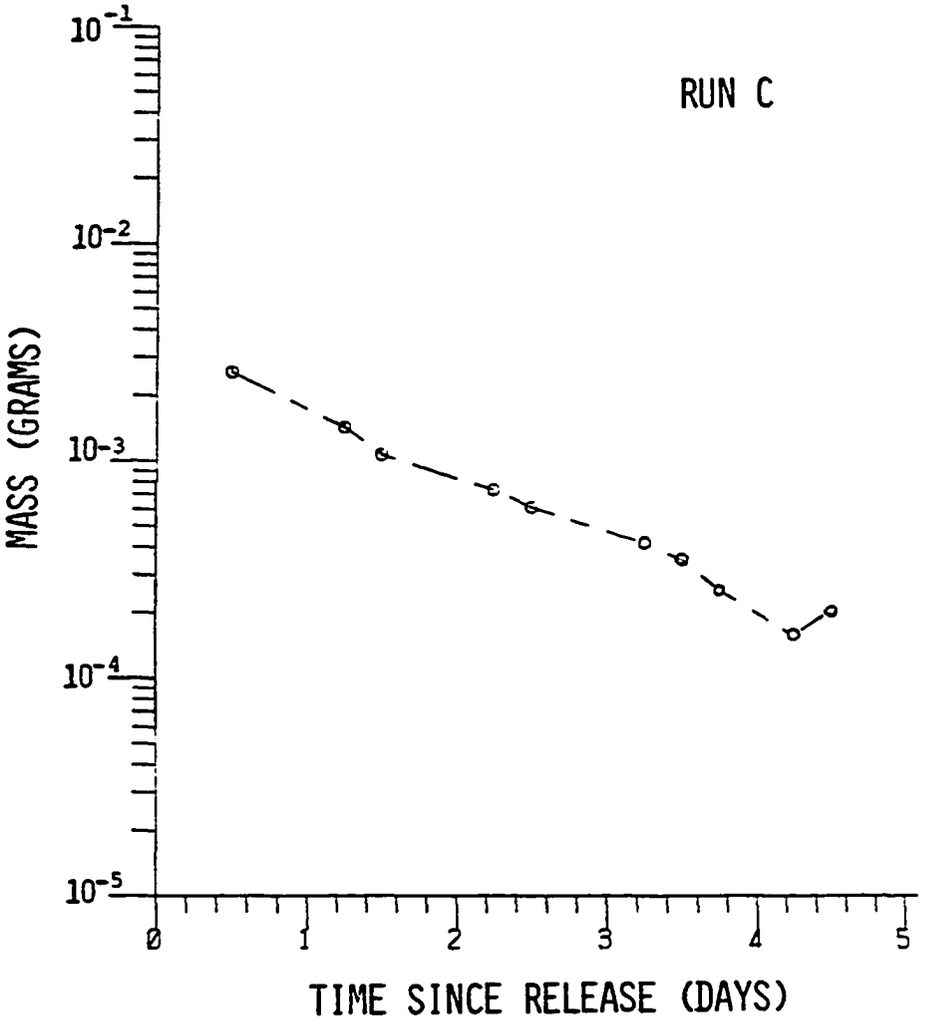

Figure 20b. Total Dye Mass in the River Versus Time in Prototype Equivalent Days since Release for Run C.

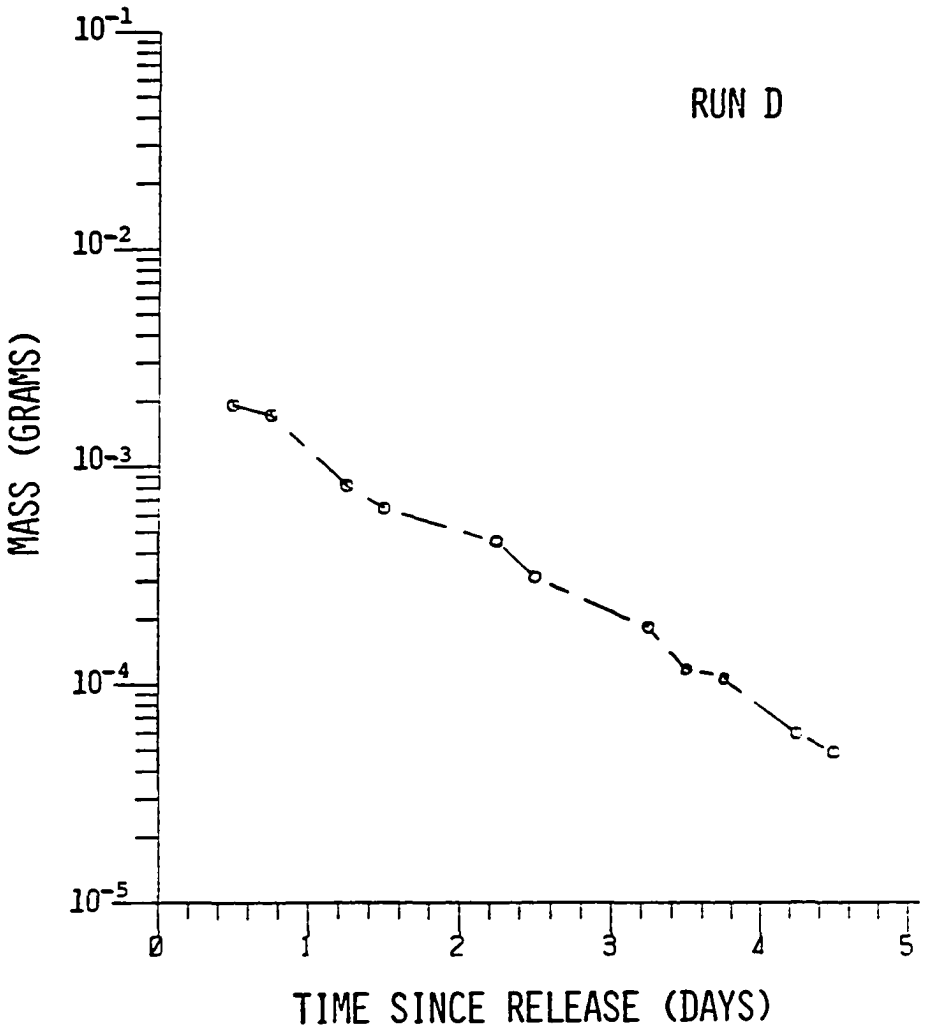

Figure 20c. Total Dye Mass in the River Versus Time in Prototype Equivalent Days since Release for Run D.

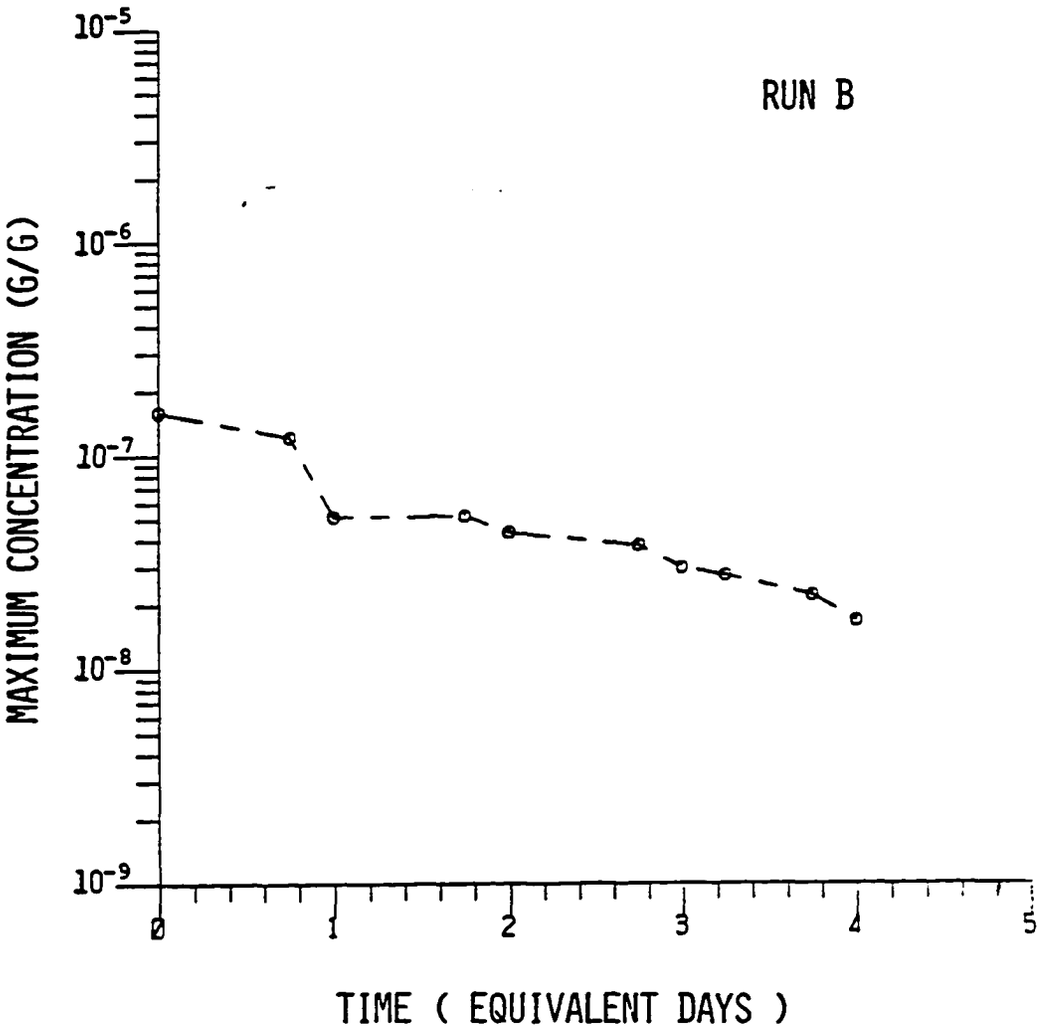

Figure 21a. Maximum Actual Dye Mass Concentration (g/g) Versus Prototype Equivalent Days fur Run B.

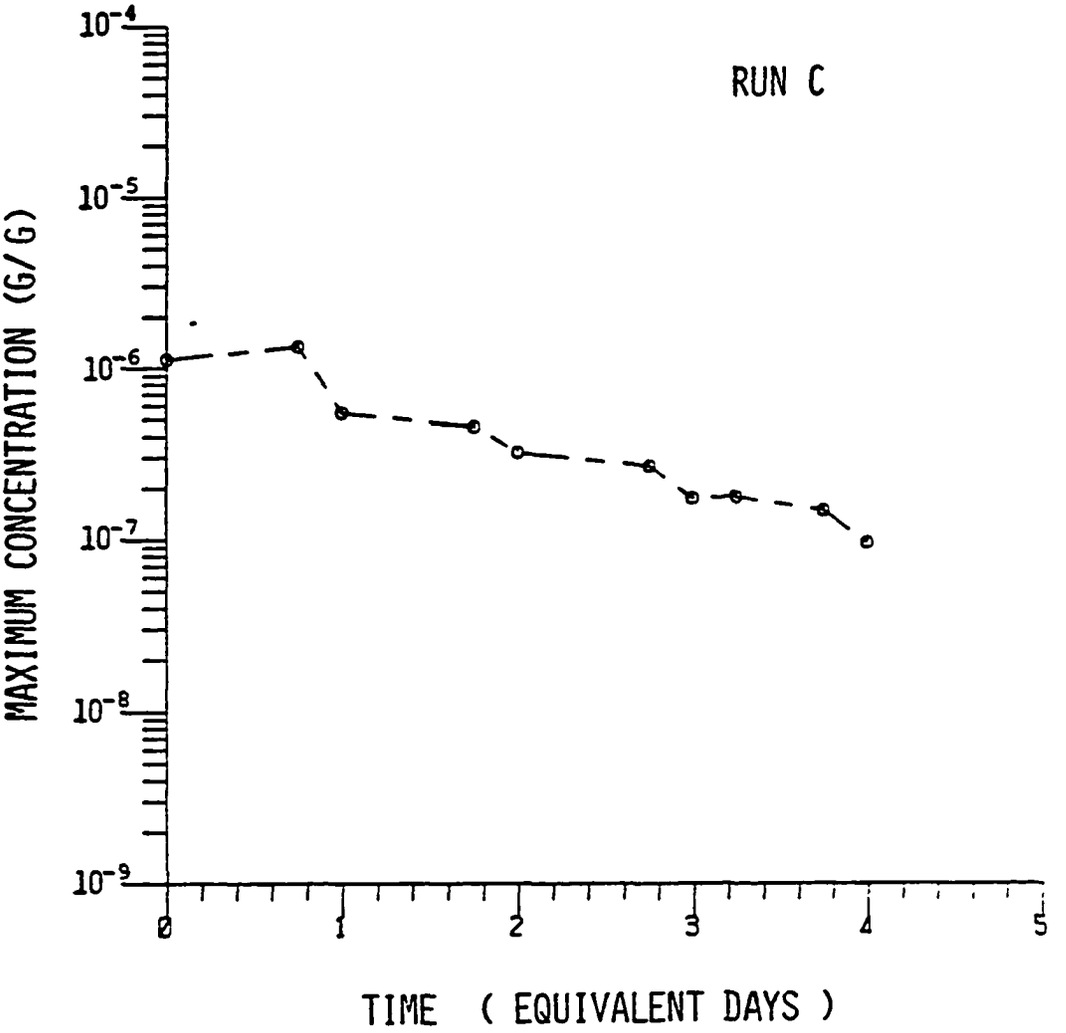

Figure 21b. Maximum Actual Dye Mass Concentration (g/g) Versus Prototype Equivalent Days for Run C.

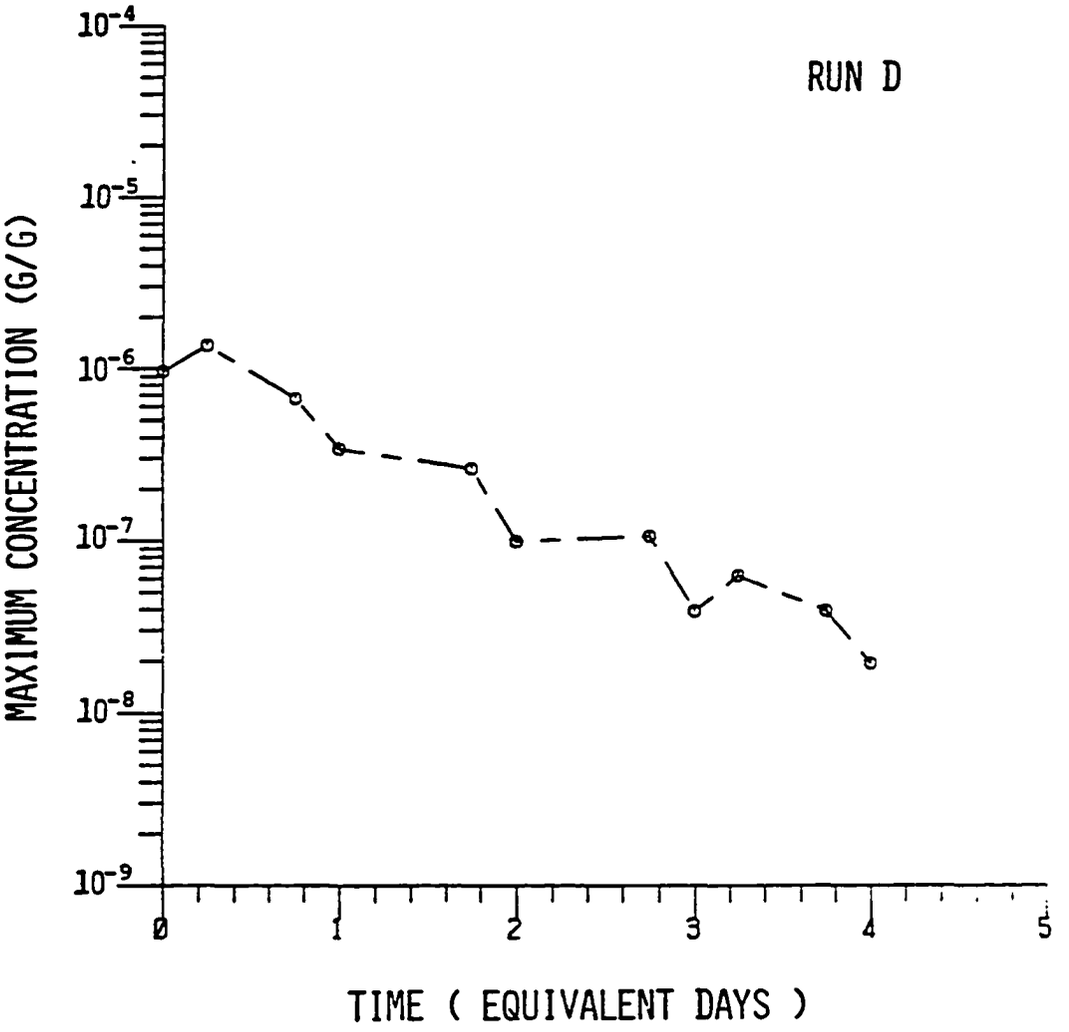

Figure 21c. Maximum Actual Dye Mass Concentration (g/g) Versus Prototype Equivalent Days for Run D.

The results for this test show that Run B and Run C are essentially the same, while Run D is substantially less. They also agree with the half-life of the total dye mass calculations. This result can be explained by looking back at the Hansen-Rattray classification model. The model results indicated that Run B and Run C were classified as type 2a estuaries, with Run C being of slightly higher stratification. Run D was classified as type 2b which is of higher stratification. Therefore,it indicates that the model went through a transition zone between the fresh water discharge rates of Runs C and D. This result is important because the Hansen-Rattray calculations work with the salinity and velocity measurements, while the half-life calculations deal with a dye tracer and yield the same results.

CHAPTER 6.

SUMMARY AND CONCLUSIONS

This investigation set out to study the effects of varying fresh water discharge on the longitudinal dispersion coefficient using the Lafayette River branch of the Chesapeake Bay Hydraulic Model. The tests were designed to simulate three different environmental conditions of normal, above normal, and heavy rainfall. The model reproduced a tide of constant tidal range and period creating a quasi-steady-state environment. Batch releases of Rhodamine WT fluorescent dye were made across the river from station L5. Surface salinity and dye samples were collected from all stations and one side embayment, with bottom samples taken from three of the deeper stations. The experimental work and analysis described in the previous chapters lead to the following conclusions.

The results from the model tests showed that as the fresh water discharge increased the model switched from well mixed for Run B, to partially mixed for Run D. This result was also seen from the vertical salinity profiles, Estuarine Richardson Number, and the Hansen-Rattray classification Model. The Hansen-Rattray Model showed good agreement between the vertical salinity profile data collected and the predicted values. The Hansen-Rattray classification model also indicated that the Lafayette River could be looked at as two separate regimes, the main channel, and the two branches. As the fresh water discharge increased, the circulation-stratification diagram indicating that the river crossed into a higher stratification classification between Run C and Run D.

There is evidence to believe that one of the major mechanisms for estuary mixing is trapping. This can be seen from Figure 13 a, where the dye concentration is stronger in the side embayment than in the adjacent stations plotted. It appears that the cross-sectional mixing was not complete until HW 6. Figure 14 shows one of the effects of trapping in that the concentrate distribution is bimodal and the main dye cloud has separated.

The dye concentrate profiles (with the concentration in g/m^3 units) show two separate distributions, one for the main channel and one for the branches. Since there appear to be two separate regimes, the entire river cannot be treated as a single one-dimensional system, but needs to be analyzed separately. Since the cross-sectional area of the river is not uniform, the data was transformed into a one-dimensional format by equation (17). The concentration profiles from this approach (Figure 15 a, b, and c) still indicate two separate regimes for the river. Due to the small amount of data from the branches, the rest of the analysis was only concerned with the main channel.

Three computational methods to calculate the longitudinal dispersion coefficient (E) were performed to study the effect of the increase in fresh water discharge on E. The salinity intrusion method showed that E varied directly with fresh water discharge. The dynamic relationship method had only a small increase of E for the low water slack approximation. E was found to be dominated by the turbulence term (E_T)with only a small effect from the local salinity term ($K\ \partial S/\partial X$). The third test for the longitudinal dispersion coefficient used the one-dimensional dye concentration distribution for the change in moment method. The values calculated from equation (24) showed that the variance did

not increase with time after the dye release indicating that cross-sectional mixing was not complete. The average values calculated from the sampling times where the variance did increase show that E remained constant with fresh water discharge for the low water slack approximation. The center of mass calculation (Figure 21) illustrates that the dye distribution migrates farther toward the mouth of the river as fresh water discharge increases. The dispersion coefficient calculated for all three methods span two orders of magnitude. Each method used a different computational model which emphasize different mixing processes. Further investigation is needed in this area to find a reason for the large spread.

The half-life of the dye mass indicates that Run B and Run C have the same flushing rate, but Run D is faster. The half-life of the maximum dye concentration, which indicates the longitudinal distribution of dye, show the same results. According to the Hansen-Rattray Model, Run D is in a higher stratification classification than Runs B and C, therefore, having a stronger salinity gradient to mix the dye.

There appears to be no simple way of determining which mechanism dominates the longitudinal dispersion coefficient from gross estuary parameters, such as the salinity and velocity fields. Further work is needed to determine which method, if any, is the correct method to calculate the dispersion coefficient. A possible answer could be found with a closer look into the concept of trapping to determine its effect on estuary mixing and dispersion.

LITERATURE CITED

Acres American Inc., 1981. Lafayette River Dye Study, Chesapeake Bay Hydraulic Model, July 1981. Columbia, Maryland.

Beltaos, S. 1978. An Interpretation of Longitudinal Dispersion Data in Rivers. Alberta Research Council. Report SWE 78-3.

____. 1980. Longitudinal Dispersion in Rivers, Journal of the Hydraulics Division. ASCE. 106:151-172.

Beltaos, S., and Day, T.J. 1978. A Field Study of Longitudinal Dispersion. Canadian Journal of Civil Engineering. 5:572-585.

Blair, C.H. 1976. Similitude of Mass Transfer Processes in Distorted Froude Model of an Estuary. Dissertation presented in partial fulfillment of the requirements for the degree of Doctor of Philosophy. Old Dominion University Department of Civil Engineering, Norfolk, Virginia.

Blair, C.H., Cox, J.H., and Kuo C.Y. 1976. Investigation of Flushing time in the Lafayette River, Norfolk, Virginia. Old Dominion University Research Foundation, Norfolk, Virginia. Technical Report 76-C4.

Blair, C.H., and Kuo, C.Y. 1979. Mass Transfer Verifications of Tidal Froude Models. Journal of the Hydraulics Division. ASCE. Technical Note Proc Paper 15016. 1561-1564.

Chatwin, P.S. 1980. Presentation of Longitudinal Dispersion Data. Journal of the Hydraulics Division. ASCE. 106:71-83.

Day, T.J. 1975. Longitudinal Dispersion in Natural Channels. Water Resources Research. Vol. 11. No. 6.

Dronkers, J. 1978. Longitudinal Dispersion in Shallow Well Mixed Estuaries. Unpublished Paper Presented at Conference on Coastal Engineering In Estuaries. Hamburg, Germany.

Farling, A.J., Blair, C.H., and Kuo, C.Y. 1976. Application of Lagrangian Dispersion Model to the Lafayette River, Norfolk, Virginia. Paper Presented to Annual Meeting of the Virginia Academy of Science.

Fisackerly, G.M. 1974. San Diego Bay Model Study, Hydraulic Model Investigation. U.S. Army Engineer. Waterways Experiment Station. Vicksburg, Mississippi.

Fischer, H.B. 1971. Analysis of the Use of Distorted Hydraulic Models for Dispersion Studies. Water Resources Research. 7:46-51.

____. 1972. Mass Transport Mechanisms in Partially Stratified Estuaries. Journal of Fluid Mechanics. 53:671-687.

Fischer, H.B., List, E.J., Koh, R.C.Y., Imberger, J., Brooks, N.H. 1979. Mixing in Inland and Coastal Waters. Academic Press. New York.

Holley, E.R., Harleman, D.R.F., and Fischer, H.B. 1970. Dispersion in Homogeneous Estuary Flow. Journal of the Hydraulics Division. ASCE. 96:1691-1709.

Harleman, D.R.F. 1971. One-Diminsional Models in Estuarine Modeling: An Assessment. (G. Ward and W. Espey, Editors). Environmental Protection Agency. Report 16070DZV.

Hudson, R.Y., Herrmann, F.A., Sager, R.A., Whalin, R.W., Keulegan, G.A., Chatham, C.E., and Hales, L.Z. 1979. Coastal Hydraulic Models. U.S. Army Corps of Engineers. Fort Belvoir, Va. Special Report No. 5.

Ippen, A.T. 1966. Estuary and Coastline Hydrodynamics. McGraw-Hill Book Company. New York.

Kuo, C.Y., Blair, C.H., Mayhew, J.D., Wong, H.F.N., and Wang, W.C. 1978. Mass Transport Study in a Hydraulic Model. Old Dominion University Research Foundation. Norfolk, Virginia.

Liu, H. 1977. Predicting Dispersion Coefficient of Streams. Journal of the Environmental Engineering Division. ASCE. 103:59-69.

Officer, C.B., and Lynch, D.R. 1981. Dynamics Mixing in Estuaries. Estuarine, Coastal and Shelf Science. 12:525-533.

Peterson, J.P., Castro, W.E., Zielinski, P.B., and Beckwith, W.F. 1974. Enhanced Dispersion in Drag Reducing Open Channel Flow. Journal of the Hydraulics Division. ASCE. 100:773-785.

Pritchard, D.W. 1967. Observations of Circulation in Coastal Plain Estuaries. In Estuaries (Editor G.H. Lauff). American Association for the Advancement of Science. 37-62.

____. 1969. Dispersion and Flushing of Pollutants in Estuaries. Journal of the Hydraulics Division. ASCE. 95:115-123.

Scheffer, N.W., Crosby, L.G., Bastian, D.F., Chambers, A.M., Granat, M.A. 1981. Verification of the Chesapeake Bay Model. Hydraulics Laboratory, U.S. Army Engineer. Waterways Experiment Station, Vicksburg, Mississippi. Tech Report HL-81-14.

Sisson, G.M. 1976. A Numerical Model for the Prediction of Tides and Tidal Currents in the Lafayette River, Norfolk, Virginia. Thesis presented in partial fulfillment of the requirements for the degree of Master of Science. Old Dominion University, Department of Oceanography, Norfolk, Virginia.

Smith, R. 1976. Longitudinal Dispersion of a Buoyant Contaminant on a Shallow Channel. Journal of Fluid Mechanics. 78:677-688.

____. 1979. Buoyancy Effects Upon Longitudinal Dispersion in Wide Well-mixed Estuaries. Department of Applied Mathematics and Theoretical Physics. University of Cambridge. Cambridge, U.K. Communicated by A.A. Townsend, F.R.S.

Sugimoto, T. 1974. Similitude of the Hydraulic Model Experiment for Tidal Mixing. Journal of the Oceanographical Society of Japan. Vol. 30. No. 6.

Taylor, G.I. 1954. The Dispersion of Matter in Turbulent Flow Through a Pipe. Proceedings, Royal Society of London. Series A. Vol. 25. No. 9. 1065-1071.

Thackston, E.L., and Krenkel, P.A. 1967. Longitudinal Mixing in Natural Streams. Journal of the Sanitary Engineering Division. ASCE. 67-90.

Thatcher, M.L., and Harleman, D.R.F. 1972. A Mathematical Model for the Prediction of Unsteady Salinity Intrusion in Estuaries. Massachusetts Institute of Technology. Com 72-10678.

Valentine, E.M., and Wood, I.R. 1977. Longitudinal Dispersion with Dead Zones. Journal of the Hydraulic Division. ASCE. 103:975-990.

Valentine, E.M. 1979. Experiments in Longitudinal Dispersion with Dead Zones. Journal of Hydraulics Division. ASCE. 105:999-1016.

Ward, P.R.B. 1974. Transverse Dispersion in Oscillatory Channel Flow. Journal of the Hydraulics Division. ASCE. 100:755-771.

White, E.G. 1972. A Physical Hydrological Study of the Lafayette River. Thesis presented in partial fulfillment of the Requirements for the degree of Master of Science. Old Dominion University, Department of Oceanography, Norfolk, Virginia.

APPENDICES

APPENDIX A

MODEL SALINITY DATA FOR THE LAFAYETTE RIVER

TABLE A-1. SURFACE SALINITY VALUES OF LAFAYETTE RIVER FOR RUN B

(UNITS: SALINITY = $^{0}/_{00}$)

SAMPLING STATIONS

EVENT	L0	L1	L2	L3	L4	L5	L5.5	L6	L7	L8S	L8N	L10N
HW 1	18.6	19.3	19.2	19.7	18.5	18.9	17.3	18.6	13.6	12.6	13.7	13.4
HW 2	19.0	19.7	19.3	19.3	19.3	19.2	16.9	18.6	13.7	12.2	13.4	13.6
LW 2	19.5	18.8	19.1	18.5	18.3	18.3	0.0	17.5	11.6	7.4	9.8	12.0
HW 4	19.3	19.8	19.5	19.6	19.2	19.3	0.0	18.6	13.4	11.1	12.4	13.4
LW 4	18.9	19.3	19.3	18.5	18.4	18.3	17.0	17.7	11.7	7.4	12.1	12.3
HW 6	20.0	20.6	20.1	20.2	19.8	19.8	17.2	19.0	13.5	11.6	14.6	13.8
LW 6	20.1	19.0	19.8	19.0	18.8	18.9	0.0	18.0	11.9	7.5	12.4	12.7
HW 8	20.3	20.4	20.4	20.4	20.0	20.3	17.3	19.3	13.7	11.0	14.4	14.2
LW 8	20.2	19.8	20.2	19.3	19.1	19.1	0.0	18.1	13.1	6.9	12.2	12.9
HW 9	19.2	20.5	19.9	19.9	19.9	20.2	17.4	19.5	15.2	11.0	15.0	14.3
HW 10	19.9	20.4	19.8	20.2	20.1	20.2	17.8	19.7	17.6	12.1	16.3	14.7
LW 10	20.0	20.0	19.9	19.3	19.2	19.3	0.0	18.5	15.6	7.6	13.3	13.1

TABLE A-2. SURFACE SALINITY VALUES OF LAFAYETTE RIVER FOR RUN C

(UNITS: SALINITY = $^{0}/_{00}$)

SAMPLING STATIONS

EVENT	L0	L1	L2	L3	L4	L5	L5.5	L6	L7	L8S	L8N	L10N
HW 1	19.6	18.7	19.0	18.8	16.0	19.8	17.1	19.6	18.3	11.2	14.7	11.8
HW 2	20.6	19.8	19.1	18.5	18.2	20.5	16.3	19.9	19.3	10.9	15.5	10.5
LW 2	20.3	19.4	18.8	17.0	16.7	18.2	0.0	16.6	11.8	4.2	10.3	7.6
HW 4	20.4	20.1	19.1	18.2	17.0	20.0	14.8	19.0	17.3	8.6	11.3	8.4
LW 4	20.1	19.4	18.9	16.6	16.0	17.9	0.0	16.2	11.4	4.1	9.4	6.7
HW 6	20.3	19.0	18.7	18.2	17.3	19.8	13.7	18.4	17.0	8.1	10.9	8.0
LW 6	20.2	18.3	18.9	16.3	15.6	17.0	0.0	14.6	10.2	3.7	9.2	6.9
HW 8	20.4	19.2	19.1	16.8	15.9	19.9	14.2	18.4	16.6	7.8	10.6	8.4
LW 8	20.6	18.5	19.0	15.9	14.7	16.8	0.0	14.7	10.1	3.5	8.8	6.7
HW 9	20.6	19.3	19.5	18.3	16.0	19.8	14.2	18.5	17.3	7.9	10.6	8.2
HW 10	20.6	19.1	19.4	16.7	16.3	20.4	0.0	0.0	17.8	9.3	13.3	8.8
LW 10	20.3	18.8	18.8	14.8	15.3	17.7	0.0	15.5	11.0	3.8	10.0	6.7

TABLE A-3. SURFACE SALINITY VALUES OF LAFAYETTE RIVER FOR RUN D

(UNITS: SALINITY = $^{0}/_{00}$)

SAMPLING STATIONS

EVENT	L0	L1	L2	L3	L4	L5	L5.5	L6	L7	L8S	L8N	L10N
HW 1	19.1	19.2	17.7	19.5	18.0	19.1	8.3	16.5	14.1	6.7	5.8	1.1
LW 2	197.	18.9	18.5	15.4	15.6	16.6	0.0	12.8	6.8	2.6	2.6	0.2
HW 3	20.0	19.7	19.7	19.1	18.2	18.9	8.5	18.2	14.0	5.5	5.8	0.2
HW 4	20.9	20.0	20.1	19.8	19.3	19.7	9.1	16.2	15.6	5.8	6.8	0.2
LW 4	19.8	19.0	17.8	16.0	15.7	15.6	0.0	12.5	6.3	2.1	2.9	0.2
HW 6	20.3	19.5	19.4	19.0	18.3	18.7	7.9	15.8	13.6	3.6	4.3	0.2
LW 6	20.1	17.5	19.5	15.1	13.9	13.4	0.0	10.7	4.4	1.5	1.9	0.2
HW 8	20.4	17.9	20.0	19.0	17.6	18.5	7.2	15.3	13.1	2.5	4.7	0.2
LW 8	20.2	19.0	19.1	14.7	13.8	14.7	0.0	11.1	4.7	1.0	1.8	0.2
HW 9	20.1	19.9	18.6	19.2	17.6	18.9	7.0	15.5	12.2	2.4	4.2	0.2
HW 10	20.4	20.6	19.8	19.8	18.9	19.8	7.1	17.5	14.4	1.7	4.4	0.2
LW 10	20.4	17.5	19.5	14.5	12.7	12.0	0.0	9.3	4.2	0.7	1.7	0.3

TABLE A-4. BOTTOM SALINITY SAMPLES FROM STATIONS L2, L4, AND L7 (UNITS : SALINITY = $^{0}/_{00}$)

	RUN B			RUN C			RUN D		
	L2	L4	L7	L2	L4	L7	L2	L4	L7
HW 1	19.2	18.7	16.3	18.9	17.2	20.2	17.6	19.3	18.2
HW 2	19.2	19.3	15.6	19.3	18.3	20.8	19.1*	19.9*	18.3*
LW 2	19.0	19.4	15.8	18.8	19.8	20.8	20.0	20.0	18.3
HW 4	19.5	19.8	17.5	19.3	20.0	20.7	20.3	20.0	18.5
LW 4	19.3	19.8	15.5	18.7	20.0	20.7	19.2	20.0	18.3
HW 6	20.2	20.4	15.8	16.5	19.3	20.6	20.0	20.1	18.3
LW 6	19.8	20.6	15.4	17.0	19.3	20.6	19.8	20.1	18.4
HW 8	20.3	20.7	15.5	17.4	19.6	20.6	20.2	20.2	18.5
LW 8	20.0	20.8	15.4	17.0	19.6	20.5	19.0	20.4	18.5
HW 9	20.0	20.5	15.2	17.4	19.3	20.2	19.7	20.4	18.4
HW 10	20.0	20.5	19.1	17.5	19.4	20.4	20.4	20.2	18.6
LW 10	19.9	20.4	20.1	18.3	19.6	20.4	20.1	20.2	00.2

* HW 3 Sampled for Run D

APPENDIX B

MODEL DYE CONCENTRATION VALUES FOR THE LAFAYETTE RIVER

TABLE B-1. ACTUAL DYE MASS CONCENTRATION (g/g) DATA

FOR RUN B ($X10^{-8}$)
SAMPLING STATIONS

EVENT	L0	L1	L2	L3	L4	L5	L5.5	L6	L7	L8S	L8N	L10N
HW 1	0.098	0.164	0.168	0.185	0.193	0.185	0.203	0.390	0.306	0.619	0.355	0.827
HW 2	0.075	0.111	0.160	0.165	0.135	0.521	19.10	0.326	0.812	0.182	4.250	1.360
LW 2	0.078	0.346	1.230	3.530	12.70	8.150	0.000	16.20	5.520	0.104	4.84	1.110
HW 4	0.354	0.183	0.487	0.632	2.720	1.950	12.50	4.670	3.270	2.900	4.240	6.270
LW 4	0.202	0.754	0.979	2.460	2.790	2.400	0.000	3.410	4.00	1.620	4.17	5.970
HW 6	0.362	0.195	0.390	0.509	0.910	0.890	4.180	1.410	1.980	2.590	2.77	6.030
LW 6	0.195	0.525	0.652	1.380	0.139	1.580	0.000	1.770	2.600	1.780	2.98	5.190
HW 8	0.189	0.234	0.364	0.341	0.567	0.472	2.460	0.923	1.340	1.700	2.21	4.620
LW 8	0.174	0.328	0.419	0.896	0.965	1.050	0.000	1.320	2.000	0.974	2.20	3.810
HW 9	0.109	0.149	0.193	0.199	0.323	0.354	1.960	0.693	1.050	1.270	1.81	3.590
HW 10	0.176	0.967	0.189	0.180	0.194	0.215	1.570	0.503	0.840	1.260	1.46	3.050
LW 10	0.135	0.176	0.226	0.636	0.651	0.694	0.000	0.795	1.430	0.635	1.64	2.510

TABLE B-2. ACTUAL DYE MASS CONCENTRATION (g/g) DATA

FOR RUN C ($X10^{-8}$)
SAMPLING STATIONS

EVENT	L0	L1	L2	L3	L4	L5	L5.5	L6	L7	L8S	L8N	L10N
HW 1	0.043	0.087	0.102	0.130	0.178	0.151	0.214	0.166	0.174	0.168	0.520	0.441
HW 2	0.052	0.055	0.063	0.081	0.072	0.110	3.500	1.350	61.20	0.064	8.390	0.485
LW 2	0.082	0.871	2.480	8.340	7.570	4.780	0.000	3.840	11.40	0.020	8.080	0.661
HW 4	0.141	0.356	0.569	1.150	2.690	1.340	1.550	2.080	4.240	2.130	6.430	6.360
LW 4	0.156	0.530	1.040	2.440	2.590	2.500	0.000	3.000	4.380	0.808	5.990	5.770
HW 6	0.208	0.261	0.467	0.596	1.060	0.880	4.710	1.360	1.860	1.110	4.140	4.860
LW 6	0.183	0.544	0.437	1.450	1.550	1.820	0.000	1.830	2.310	0.411	3.370	3.670
HW 8	0.181	0.241	0.296	0.395	0.650	0.531	2.270	0.864	1.160	0.802	2.290	3.120
LW 8	0.171	0.346	0.320	0.903	0.952	1.050	0.000	1.140	1.440	0.360	1.890	2.180
HW 9	0.168	0.164	0.177	0.283	0.466	0.373	1.540	0.660	0.740	0.600	1.630	2.220
HW 10	0.181	0.107	0.178	0.189	0.304	0.208	1.290	0.458	5.440	0.604	1.450	1.920
LW 10	0.145	0.228	0.288	0.574	0.574	0.610	0.000	0.679	1.020	0.203	1.320	1.400

TABLE B-3. ACTUAL DYE MESS CONCENTRATION (g/g)

FOR RUN D ($X10^{-8}$)
SAMPLING STATIONS

EVENT	L0	L1	L2	L3	L4	L5	L5.5	L6	L7	L8S	L8N	L10N
HW 1	0.048	0.112	0.113	0.138	0.164	0.148	0.205	0.176	0.162	0.085	0.000	0.248
LW 2	0.104	1.330	0.731	5.220	9.770	4.080	0.000	1.690	7.840	0.039	0.825	0.083
HW 3	0.200	0.418	0.203	1.290	4.850	1.440	13.80	2.020	3.740	4.240	9.210	0.041
HW 4	0.366	0.192	0.195	0.600	1.380	0.701	6.850	1.480	1.780	2.920	6.820	0.029
LW 4	0.210	0.765	0.694	1.580	1.870	1.500	0.000	1.480	2.040	0.907	3.630	0.030
HW 6	0.198	0.304	0.319	0.500	0.877	0.617	2.800	0.962	1.130	0.607	2.020	0.027
LW 6	0.173	0.540	0.388	0.825	1.130	0.983	0.000	0.811	0.741	0.203	1.080	0.028
HW 8	0.175	0.198	0.186	0.212	4.390	0.394	1.230	0.540	0.569	0.202	1.010	0.038
LW 8	0.168	0.199	0.212	0.444	0.529	0.497	0.000	0.406	0.389	0.139	0.404	0.029
HW 9	0.175	0.163	0.191	0.185	0.300	0.198	0.791	0.416	0.360	0.180	0.732	0.032
HW 10	0.152	0.123	0.152	0.159	0.143	0.182	0.557	0.305	0.325	0.156	0.591	0.046
LW 10	0.150	0.198	0.186	0.228	0.336	0.314	0.000	0.200	0.203	0.075	0.229	0.081